# Development and Evaluation of a Test Apparatus for Fuel Cells

Mark William Davis

Thesis submitted to the faculty of the
Virginia Polytechnic Institute and State University
in partial fulfillment of the requirements for the degree of

Master of Science

in

Mechanical Engineering

Dr. Michael Ellis, Chair
Dr. Michael R. von Spakovsky
Dr. Douglas J. Nelson

May 25, 2000
Blacksburg, Virginia

Keywords: Fuel Cell, PEM, Test Apparatus, Experimental

# Development and Evaluation of a Test Apparatus for Fuel Cells

Mark William Davis

## ABSTRACT

The development of a test apparatus for proton exchange membrane fuel cells is presented. The design of the prototype device is provided in detail along with a description of the apparatus. The evaluation of the functionality and effectiveness of the device included measurement of a polarization curve for a 5-cell, 1 kW stack. An effective test apparatus is imperative for stack performance testing, model evaluation, and investigation of new fuel cell technology. This apparatus was designed to measure and control the mass flow rates of the reactant gases, gas pressures, gas temperatures, gas relative humidity, stack temperature, stack current, and the coolant water flow rate. Additionally, the test apparatus can measure the stack voltage, coolant water resistivity, coolant water temperature change across the stack, and the coolant water pressure drop across the stack. The apparatus was shown to provide adequate control of all necessary variables for stack performance evaluation.

## DEDICATION

Praise and glory and wisdom and thanks and honor and power

and strength be to our God for ever and ever. Amen

Rev 7:12

## ACKNOWLEDGEMENTS

I want to thank my advisor, Dr. Mike Ellis, for his guidance and instruction, as well as his consideration and understanding of my schedule. This work would not have been possible without the generosity of Ingersoll-Rand and Energy Partners, Inc. Financial support was provided by the Virginia Tech Aspires program, the Gate Center, and the Pratt Foundation. Additionally, I would like to thank Dr. W.C. Thomas for lending his equipment and expertise to the project. I also appreciated the assistance of Todd Walter, Morgan Stewart, Frank Lomax, and Burak Gunes.

Finally, I need to thank my wife, Christy, whose love and support inspired me to persevere.

# NOMENCLATURE

## *Variables*

A = inside area of tube

$c_{p_i}$ = specific heat of gas

$d$ = inside diameter of tube

F = Faraday's constant

$h_i(T)$ = specific enthalpy of ideal gas at temperature, T

$h_{H_2O,g}(T)$ = specific enthalpy of gaseous water at temperature, T

$h_{H_2O,f}(T)$ = specific enthalpy of liquid water at temperature, T

$M_i$ = molecular weight of molecule

$\dot{m}_i$ = mass flow of gas (air, hydrogen, or nitrogen)

n = number of electrons

$SR_i$ = stoichiometric ratio of gas in stack (air or hydrogen)

P = power produced by stack

$P_i$ = pressure of gas

$p_v$ = partial pressure of water vapor in gas mixture

$p_{sat}(T)$ = saturation pressure of water at the temperature, T

$Q$ = heat transfer from heater to gas

$\dot{Q}$ = heat transfer rate

$R_i$ = universal gas constant for specified gas

SLPM = standard liters per minute

$T_i$ = temperature of gas

$V_i$ = velocity of gas in tube

$V_c$ = voltage of each cell in stack

$V_{reservoir}$ = volume of water in reservoir

$\dot{V}$ = volumetric flow rate

$\Delta P$ = pressure drop of gas in tube

$\Delta T$ = temperature difference between heater outlet and inlet

$\rho_i$ = density of gas

$\mu_i$ = viscosity of gas

$\omega$ = absolute humidity ratio of gas

$\Phi$ = relative humidity of gas

## *Subscripts*

*fci* = fuel cell inlet

*o* = source

*i* = either hydrogen or air

# TABLE OF CONTENTS

**ABSTRACT** ..... **II**

**DEDICATION** ..... **III**

**ACKNOWLEDGEMENTS** ..... **IV**

**NOMENCLATURE** ..... **V**

VARIABLES ..... V
SUBSCRIPTS ..... VI

**TABLE OF CONTENTS** ..... **VII**

**1 INTRODUCTION** ..... **1**

**2 LITERATURE REVIEW** ..... **3**

2.1 ANALYTICAL MODELS ..... 4
2.2 EMPIRICAL MODELS ..... 6
2.3 EXPERIMENTAL DATA ..... 8
2.4 IMPORTANT OPERATING PARAMETERS ..... 9
2.5 RESEARCH GOALS ..... 10

**3 TEST APPARATUS DESIGN** ..... **11**

3.1 DESIGN CRITERIA ..... 11
*3.1.1 Sizing Requirements* ..... *12*
3.1.1.1 Gas mass flows ..... 13
3.1.1.2 Temperature ..... 14
3.1.1.3 Pressure ..... 14
3.1.1.4 Humidity ..... 15
*3.1.2 Control Requirements* ..... *15*
3.1.2.1 Computer controls ..... 15
3.1.2.2 Manual controls ..... 15
3.1.2.3 Safety overrides ..... 16
3.2 SYSTEM DESIGNS ..... 16
*3.2.1 Fuel and Oxidant Gases* ..... *16*
3.2.1.1 Mass Flow ..... 18
3.2.1.2 Temperature ..... 19
3.2.1.3 Pressure ..... 19
3.2.1.4 Humidity ..... 21
*3.2.2 Coolant Water* ..... *26*
3.2.2.1 Flow ..... 27
3.2.2.2 Temperature ..... 28
3.2.2.3 Purity ..... 29
*3.2.3 Load* ..... *29*

*3.2.4 Measurement/Control* ..... *29*

**4 TEST APPARATUS CONSTRUCTION ..... 31**

4.1 BASIC MATERIALS ..... 31
4.2 LAYOUT ..... 31
*4.2.1 Fuel* ..... *33*
*4.2.2 Oxidant* ..... *35*
*4.2.3 Coolant* ..... *36*
*4.2.4 Load* ..... *37*
*4.2.5 Measurement/Control* ..... *37*
4.3 ASSEMBLY ..... 38
*4.3.1 Fuel and Oxidant* ..... *39*
4.3.1.1 Common Devices ..... 39
4.3.1.2 Fuel System Components ..... 43
4.3.1.3 Oxidant System Components ..... 43
*4.3.2 Coolant System Components* ..... *44*
4.3.2.1 Coolant reservoir (C-1) ..... 45
4.3.2.2 Heater (C-1b) ..... 45
4.3.2.3 Pump (C-3) ..... 46
4.3.2.4 Flow Meters (C-11 and C-11a) ..... 46
4.3.2.5 Resistivity Transmitter (C-6) ..... 47
4.3.2.6 In-Line Deionizer (C-7) ..... 47
4.3.2.7 Water Filter (C-8) ..... 47
4.3.2.8 Heat Exchanger (C-9) ..... 48
4.3.2.9 Level Sensor (C-1a) ..... 48
4.3.2.10 Differential Temperature Meter (C-12) ..... 48
4.3.2.11 Control Valve (C-10) ..... 49
*4.3.3 Load System Components* ..... *49*
*4.3.4 Measurement/Control Components* ..... *50*
4.3.4.1 Control Devices ..... 51
4.3.4.2 Measurement Devices ..... 52
*4.3.5 Safety System Components* ..... *53*
4.3.5.1 Hood ..... 54
4.3.5.2 H2 Alarms ..... 54
4.3.5.3 Nitrogen Purge ..... 54
4.3.5.4 Flashback Arrestor ..... 54

**5 TEST APPARATUS EVALUATION ..... 55**

5.1 COMPONENT EVALUATION ..... 55
*5.1.1 Pressure Transducers* ..... *55*
*5.1.2 Relative Humidity Transmitter* ..... *55*
*5.1.3 Mass Flow Meters* ..... *56*
*5.1.4 Resistivity Transmitter* ..... *56*
*5.1.5 Differential Temperature Meter* ..... *56*
*5.1.6 Level Switch* ..... *56*
5.2 SYSTEM EVALUATION ..... 57
*5.2.1 Fuel* ..... *57*

*5.2.2 Oxidant* ..... *58*
*5.2.3 Coolant* ..... *58*
*5.2.4 Load* ..... *60*
*5.2.5 Safety* ..... *61*
5.3 PERFORMANCE EVALUATION ..... 61
**6 CONCLUSION/RECOMMENDATIONS ..... 65**
**REFERENCES ..... 67**
**APPENDIX 1 – SYSTEM DRAWINGS ..... 69**
**APPENDIX 2 – PARTS LIST ..... 80**
FUEL SYSTEM ..... 80
OXIDANT SYSTEM ..... 81
COOLANT SYSTEM ..... 82
**APPENDIX 3 – OPERATING PROCEDURE ..... 83**
**VITA ..... 89**

# 1 INTRODUCTION

The world has been searching for an inexpensive, efficient, and practical renewable energy source for the past few decades. Fuel cells, although they have existed for more than 50 years, are just starting to capture the interest of the general public. Fuel cells promise clean and efficient operation along with high energy densities. While there are many different types of fuel cells, the proton exchange membrane fuel cell stands out as one of the most promising for transportation and small stationary applications.

Proton exchange membrane (PEM) fuel cells take hydrogen and air and produce power and water. The mechanism is exactly opposite to that of electrolysis. In electrolysis, an electric current is run through water and the water reacts to form hydrogen and oxygen. PEM fuel cells take hydrogen and split it into protons ($H^+$) and electrons. The $H^+$ molecules diffuse across a polymer membrane, and the electrons travel through the load circuit. Those electrons join with the diffusing proton on the other side of the membrane and react with oxygen to form water. The electro-chemical reactions are shown below along with a schematic of a PEM fuel cell.

Anode reaction: $H_2 \rightarrow 2H^+ + 2e^-$

Cathode Reaction: $\frac{1}{2}O_2 + 2H^+ + 2e^- \rightarrow H_2O$

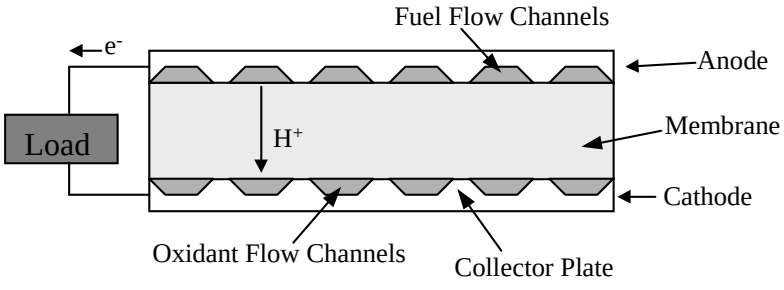


**Figure 1-1. PEM fuel cell schematic**

Fuel cell research has increased greatly over the past decade. A number of

corporations are attempting to develop powerful, efficient, low cost, and marketable PEM fuel cells. Membrane chemistry and catalyst loading continue to develop, and, as they do, the power density and efficiency of the cells increase. Therefore, as the technology continues to mature, a need arises for the ability to experimentally test the developing technology and better understand the present technology

The goals of this research are to design and construct a prototype test apparatus, to apply the apparatus to develop a fuel cell polarization curve, and to evaluate the prototype to determine any modifications or enhancements, which would improve its flexibility, control, and accuracy.

# 2 LITERATURE REVIEW

The construction of an effective proton exchange membrane fuel cell (PEMFC) test apparatus requires knowledge of the important physical parameters that affect the performance of PEMFCs. Also, because precise control of operating conditions is difficult and expensive, an idea of the key parameters to control for effective performance evaluation is required. This was accomplished by observing commercially available fuel cell test apparatus, descriptions of apparatus used to obtain published experimental data, and published fuel cell performance models and the variables that they emphasized.

The advancement of fuel cell technologies in the last decade has produced a wealth of investigative studies into the prediction of fuel cell performance. The prediction of PEMFC performance has been of particular interest due to their suitability for the transportation industry. The prediction of fuel cell performance is key in the development of new applications. A simple, effective, and accurate model of overall fuel cell performance would ease the design of new fuel cell applications.

Unfortunately, the performance of a PEMFC is extremely difficult to model analytically. Its performance depends on many variables. These include temperature, pressure, current, water content of the membrane, stoichiometry of the inlet gases, etc. Additionally, many of the variables that influence performance depend on each other yielding non-linearities in the performance models. The presence of these non-linear equations and the difficulty in quantifying some of the important performance variables (membrane characteristics, diffusion coefficients, etc.) has lead some researchers to establish empirical models of PEMFC performance. In general, however, these models are only accurate over small ranges of operating conditions. Both analytical and empirical models require experimental data. The empirical model uses the measured data to fit the fuel cell's performance to a prescribed equation form, and the analytical model depends on experimental data to investigate the model's accuracy.

Proton exchange membrane fuel cells are highly complicated systems. The measure of performance most often associated with PEMFCs is a polarization curve,

which describes the output voltage over a range of current densities for a specific set of operating conditions. The operating voltage is governed by the thermodynamic equilibrium potential and the losses in the system. The equilibrium potential is a function of the temperature, pressure, fuel concentration, oxidant concentration, and several equilibrium constants. The losses are separated into two main categories. First, the activation overvoltage is the result of losses in the reaction kinetics, thermodynamics, and mass transfer. The second major loss is referred to as the ohmic overvoltage. Ohmic overvoltage depends on the resistance to proton flow across the membrane and the resistance to electron transfer in the porous electrodes. Each of the losses depends on the temperature, pressure, current, gas concentrations, design parameters, and materials of construction. The interdependence of many of the performance variables creates difficulties in detailed, accurate models. Therefore, an effective test apparatus must have the ability to precisely measure all of the parameters that influence fuel cell performance.

## *2.1 Analytical Models*

The complexity of fuel cell operation yields extremely complex mathematical models if every factor involved in the performance is considered. But, an analytical model is preferred to a simpler empirical model. If an accurate analytical model could be formulated, it would be adaptable to different conditions and, more importantly, to different fuel cells (if the appropriate parameters were known). An empirical model is only valid for those fuel cells for which it is created. To ease the difficulty of modeling the entire fuel cell, major assumptions are made.

There are a large number of analytical models in the literature. Several representative models were reviewed in order to establish the most significant operating parameters and to provide a basis for interpretation of the experimental results. The cell voltage depends on the reversible cell voltage and the losses associated with mass transport, reaction kinetics, electron transfer, and proton diffusion. The difference between models lies in their approximation of these relations. The variables that are included in each model and the impact of each variable are considered.

The model proposed by Nguyen and White (10) investigates the two-dimensional

heat and mass transfer across the membrane electrode assembly including the flow channels on either side. The governing equations for the model include effects from the reactant gas mass flows, temperature, pressure, and relative humidity, and the current. Thirumalai and White (13) performed a sensitivity analysis on the model derived by Nguyen and White (10) to determine the most important of these parameters. The model was run at galvanostatic conditions with a current density of 0.6 $A/cm^2$. The study found that the gas mass flows, the operating pressure, and the operating temperature were the most important variables in fuel cell performance. They also noted that the anode relative humidity, not the cathode relative humidity, had a large impact on the performance. A model proposed by Yi and Nguyen (14) is similar to the Nguyen and White model, but Yi and Nguyen develop a more complete description of the solid layer temperature that can be used to analyze the effect of heat exchanger parameters and the inlet coolant temperature. These models, as do all analytical models, require extensive experimental data to validate the accuracy of the model. The apparatus that would be used to verify models such as these would need to accurately measure the variables mentioned above.

A model by Springer et al. (12) concentrated on a fuel cell's performance depending on the concentration of water in the membrane electrode assembly. The model accounted for the cell current, the cell temperature, the humidifier temperature, which determines the relative humidity of the inlet gases, the inlet gas pressures and flow rates, and the partial pressure of oxygen in the cathode gas stream. The model by Bernardi and Verbrugge (4) closely resembles the Springer et al. model, but the Bernardi and Verbrugge model accounts for the presence of liquid water in the flow channels and the diffusion of water across the membrane as a result of the pressure difference between the anode and cathode. Although the apparatus will not have the capability to measure the actual water content of the membrane, it must provide measurement of the inlet parameters including the temperature, pressure, and relative humidity that may determine the water content.

Marr and Li (9) start by defining the open circuit voltage as a function of the operating temperature and the reactant partial pressures. They use a set of differential

equations to define the electrochemical reaction, mass transfer, and the ohmic losses in the catalyst layers. These relations depend on the operating temperature and the reactant concentrations, which can be related to their respective partial pressures. In the membrane, they assume a constant proton concentration, and their expression relates the membrane resistive loss to the proton concentration and the pressure differential across the membrane. In the electrodes, the model accounts for the resistance of the bi-polar plates. Finally, the reactant and product concentrations are taken into account in the flow channels. Overall, the model formed by Marr and Li relates fuel cell performance to the operating temperature, the reactant partial pressures, and the electrical resistance.

Amphlett et al. (1), like Marr and Li, relate the open-circuit voltage to the operating temperature and the reactant partial pressure. They use the Butler-Volmer equation and an expression for the exchange current to derive expressions for the anodic and cathodic activation overvoltages that depend on the temperature, oxygen concentration, and the current. They define the ohmic resistance losses as a sum of the losses from electron transfer through the electrode and proton transfer across the membrane. They also consider proton transfer due to an electrical potential gradient, a proton concentration gradient, and convection of protons associated with the diffusion of water. Amphlett et al. (1) take great care to derive the ohmic resistance of the membrane with respect to the proton concentration, temperature, and current. They state that there is also an effect of the water concentration on the membrane resistance, but they admit that limited understanding of the phenomenon prevents its specific inclusion in the model. The final expression for the ohmic losses is so complicated that the author proposes using the analytical model only to gain an insight into the important variables required to create an effective empirical model.

## *2.2 Empirical Models*

Although empirical models are not the preferred method of predicting fuel cell performance, they are much simpler to create accurately than the analytical models. Empirical models are created by establishing a relation for the output voltage that depends on a few selected performance variables (such as temperature, pressure, relative humidity, and current) and a number of constants. The variables that the different

modelers use and the success of their models helps to determine the measurements and controls required for the test apparatus. The numerical values for the constants are established by fitting the empirical relation to a set of experimental data. The reliance on experimental data is one reason that the analytical models are preferred over empirical models. Every fuel cell is different, and using experimental data to establish a performance model limits that model to the fuel cell from which the experimental data came. Also, the model is only as accurate as the number of performance variables included in the empirical equation. If a variable is omitted from the equation, the empirical relation is only valid when the omitted variable has the value equal to that at which the experimental data was collected.

The empirical model developed by Amphlett et al. (2) attempts to broaden the limitations of the empirical model to include all operating conditions. Amphlett et al. (2) use the relations for the output voltage developed in the analytical model to expand the scope of their empirical model. The difficulty with the Amphlett et al. analytical model (1) was in the determination of the activation overvoltage and the ohmic overvoltage. They established that the activation overvoltage was dependant on the temperature, current, and the oxygen concentration, and they knew that the expression for the ohmic overvoltage included some function of temperature and current. They implemented an experimental plan to statistically determine the necessary constants for the two expressions.

Lee and Lalk (8) implemented a different type of empirical model to evaluate fuel cell performance. Their model used an empirical relation to define the fuel cell output voltage using only the cell current. The empirical equation was established at a number of different operating conditions on a laboratory scale stack. The model uses this relation to approximate larger, more useful stacks. The Lee and Lalk (4) model used a finite difference scheme along the gas channels of the fuel cell to determine the temperature at each element. Using this temperature and the empirical voltage relation, and an estimate of the stack voltage, the program iteratively finds the current. The calculated power and the desired power are compared, and the process starts again with a new estimate of the voltage.

Barbir et al. (3) used an even simpler empirical model to determine fuel cell performance. They recognized that the output voltage is best modeled with an empirical equation dependant on the current density, the logarithm of the current density, and the exponential of the current density, but they estimated the polarization curve for a fuel cell as a linear function of the current density over the range of operating conditions normally used. The linear equation was based on experimental results for polarization curves at different operating pressures.

## *2.3 Experimental Data*

Specific information about the apparatus used in obtaining experimental data for verification of the above models and others like them is not available. A few authors provided brief descriptions of a few fuel cell test apparatus. The apparatus used by Amphlett et al. (1,2) to acquire the experimental data was able to control the mass flow and the partial pressure of the reactant gases. The hydrogen and oxygen were supplied with compressed gas tanks, and the partial pressures were adjusted by combining the gases with carbon dioxide and nitrogen respectively. The temperature of the stack was controlled by the circulating water. Current measurements on the stack were made with a 50 Amp shunt. Lee and Lalk (8) indicated that their test apparatus could measure the gas temperatures, pressures, mass flows, and humidities, the coolant temperature and flow rate, the stack current and voltage, the cell temperatures and voltages, and the outlet air temperature and pressure. All of these variables were viewed as necessary for determining the performance of a fuel cell stack.

An investigation into the effect of carbon monoxide concentrations in the fuel stream was performed by Oetjen et al. (11) using a “homemade” test apparatus that could control the reactant mass flows, temperatures, and pressures. It was also capable of varying the load placed on the stack in order to determine polarization curves for a stack. A cathode model of a fuel cell by Broka and Ekdunge (5) used a test apparatus with a temperature-controlled humidification system of the reactant gases, control of the cell temperature, and mass flow control of the reactant gases. By observing the test apparatus constructed by other fuel cell researchers, it was determined that control of all aspects of the inlet reactant gases, cell temperatures and voltages, coolant temperature and flow rate,

and load current and voltage are necessary for analytical model verification and empirical studies.

A small number of test apparatus are commercially available today. The most comprehensive model is produced by Hyrogenics. Their Fuel Cell Automated Testing System (FCATS) can test fuel cell stacks up to 12 kW (7). The FCATS can control the mass flows up to 700 SLPM for the fuel and 1000 SLPM for the oxidant, temperatures up to 95°C, pressures up to 40 psig, and relative humidities up to 100 percent. The stack temperature is maintained using a cooling fluid, which is heated during start-up. The inlet cooling fluid can be controlled from 20°C to 95°C. A programmable load can draw 100V, 1000A, and 12 kW with a constant current, voltage or resistance. The system is computer controlled. It measures all inlet mass flows (reactant gases and coolant fluid), the reactant pressures and their corresponding differential pressures across the stack, stack pressure, inlet and outlet temperatures for the reactant gases and the coolant fluid, stack temperature, cooling fluid resistivity, up to 32 cell voltages, the stack voltage, and the stack current. Additionally, the device can simulate reformate gases that consist of hydrogen, carbon dioxide, carbon monoxide, nitrogen, and air. Finally, the FCATS can measure the amount of water leaving both the anode and cathode outlets of the stack.

ElectroChem, Inc. produces the FC Lab, which can measure the stack voltage, current, power, resistance, fuel flow rates, and temperatures (6). The apparatus can control the anode and cathode gas channels. Like the FCATS, it can also simulate reformate gases. The FC Lab can easily perform a Tafel, profile, or shock test on a fuel cell stack, and it can drive the fuel cell under operator-programmable dynamic load conditions.

## *2.4 Important Operating Parameters*

A study of the different models and the experimental apparatus presented here reveals some consistent themes. All of the models suggested that the performance of fuel cell stacks depend on the operating temperature, pressure, relative humidity of the inlet gas streams, and the current. All of the experimental apparatus were able to control the temperature and mass flow of the reactant gases. Most devices had the capability to

adjust the reactant pressures and relative humidities as well. A few select fuel cell test apparatus could control the stack temperature and the makeup of the fuel gas. Overall, the success of a PEMFC test apparatus relies on the control of the operating temperature, pressure, relative humidity, reactant mass flows, and current.

## *2.5 Research Goals*

The primary goal of this research is to design and construct a fuel cell test apparatus with the capability to control and measure all of the necessary parameters for effective PEMFC research. A review of PEMFC literature has indicated those parameters, and the design of the test apparatus will reflect the information gathered from the literature

# 3 TEST APPARATUS DESIGN

The proton exchange membrane fuel cell test apparatus at Virginia Tech is intended to facilitate research into the performance of PEM fuel cells and to characterize newly developed fuel cell prototypes. The specific criteria used to design the apparatus are outlined in the following section

## *3.1 Design Criteria*

A greater understanding of fuel cells and their performance can be achieved if fuel cell inputs and output are precisely controlled and measured. This test apparatus is designed to control:

- Reactant gases
  - flow rate
  - temperature
  - pressure
  - relative humidity
- Coolant water
  - temperature
  - pressure
  - flow rate
  - resistivity
- Electrical load.

Experimental fuel cell research, characterization, and modeling can be pursued with a test apparatus that can control all of these variables.

### 3.1.1 Sizing Requirements

The test apparatus is designed to test proton exchange membrane fuel cells capable of producing 5 kW or less. Although a fuel cell of this power output is not necessarily useful in most practical applications, fuel cells are modular so that the performance of a relatively small stack can be accurately scaled up to represent the performance of a larger stack. Designing the test apparatus for a smaller stack makes the design of the apparatus easier and cheaper because smaller components can be bought or manufactured.

Requirements for the other operating parameters can be prescribed based on the maximum power output of 5 kW. Size requirements must be set for the gas mass flows, gas temperatures, the fuel cell operating temperature, gas pressures, gas humidity levels, and coolant water flow rate. The criteria for the nitrogen flow rate and the minimum resistivity of the water are recommended by the manufacturer for operation of the PEM fuel cell stack tested. Also, a minimum power requirement must be established to easily and accurately measure and control certain quantities. This minimum is highly dependent on the ranges of the major measuring and control devices. Table 3-1 shows the minimum and maximum design criteria, and these criteria are discussed in more detail in the following sections.

**Table 3-1. Design Criteria for PEM Fuel Cell Test Apparatus**

| Criteria | Minimum | Maximum |
|---|---|---|
| **Power** | 0.1W | 5000 W |
| **Mass Flow** | | |
| $H_2$ | 0.8 SLPM | 170 SLPM |
| Air | 2 SLPM | 500 SLPM |
| $N_2$ | 0.27 SLPM per cell | |
| Water | 2 LPM | 20 LPM |
| **Temperature** | Room | 80° C |
| **Pressure** | Atmospheric | 400 kPa gauge |
| **RH** | | |
| $H_2$ | 0% | 95% |
| Air | 25%* | 95% |
| **Resistivity** | 2 Mohm-cm | 20 Mohm-cm |

* Minimum relative humidity depends on compressor tank humidity and system pressure

#### 3.1.1.1 Gas mass flows

The mass flow for both the fuel and oxidant gas are dependent on the power produced by the fuel cell. As the load draws current from the stack, the hydrogen reacts at the electrode-membrane interface (i.e. in the catalyst layer) by splitting into hydrogen protons and electrons, and because current is a measure of the flow of electrons, the hydrogen mass flow is directly related to the current. The actual mass flow of hydrogen depends on the current and the stoichiometry on the anode side of the fuel cell. The test apparatus will typically run hydrogen dead-ended, which corresponds to a stoichiometric ratio of exactly 1. But, to provide for flexibility in operation, a stoichiometric ratio of two is used as the design criteria. The following calculation determines the maximum hydrogen flow rate.

$$\dot{m}_{H_2} = \frac{P * SR_{H_2} * M_{H_2}}{n * F * V_c} \tag{1}$$

where,

$P$ = the maximum power for the apparatus (5000W),

$SR_{H_2}$ = the design stoichiometric ratio for hydrogen (2),

$M_{H_2}$ = the molar weight of hydrogen (2 g/gmol),

$n$ = the number of electrons (2),

$F$ = Faradday's constant (96484 C/mol), and

$V_c$ = the design cell voltage (0.5V).

In this calculation, it is assumed that the minimum voltage at which a cell would operate is 0.5V. The maximum mass flow rate for hydrogen is calculated to be 152 SLPM. A similar computation relates the current and the oxygen mass flow rate. Typically, the air stoichiometric ratio ranges from 2 to 2.5. The following calculation results in a maximum air mass flow rate of 453 SLPM.

$$\dot{m}_{Air} = \frac{1}{2} * \frac{4.76 * M_{Air} * P * SR_{Air}}{n * F * V_c} \quad (2)$$

where,

$P$ = the maximum power for the apparatus (5000W),

$SR_{Air}$ = the design stoichiometric ratio for air (2.5),

$M_{Air}$ = the molar weight of air (28.97 g/gmol),

$n$ = the number of electrons (2),

$F$ = Faradday's constant (96484 C/mol), and

$V_c$ = the design cell voltage (0.5V).

The minimum mass flow criteria are established by the range of the mass flow controllers. The controllers purchased are capable of metering flows greater than 2 percent of full scale. This condition resulted in minimum flows of 0.8 SLPM for the fuel system and 2 SLPM for the oxidant system.

#### 3.1.1.2 Temperature

The temperature requirements of the fuel cell test apparatus depend on the stack itself. Each stack and membrane have specific temperature limits. These limits have impacts on the type of material used in construction of the test apparatus and on the capabilities of the heaters and humidifiers. Typical PEM fuel cells operate in the range of 60-80°C. For design purposes, an upper limit of 80°C for the water leaving the fuel cell and for the inlet gases was used. The minimum temperature criteria is established by the lack of refrigerated cooling capability, and, therefore, the minimum temperature achievable is room temperature (approximately 22°C).

#### 3.1.1.3 Pressure

The pressure requirements have a similar logic to the temperature requirements mentioned above. The typical pressure limit for PEM fuel cells is approximately 400 kPa

gauge. Similar to the temperature criteria, the minimum pressure is atmospheric pressure. However, the minimum working pressure is determined by the individual fuel cell and the pressure drop associated with the gas streams flowing through the stack.

#### 3.1.1.4 Humidity

The water balance of a fuel cell is one of the most difficult obstacles to overcome. The addition of too little water to the gas streams can dry the membranes and cause serious damage. On the other hand, too much water in the gas streams can lead to flooding in the membrane, which prevents the transport of gas to the reaction sites and limits performance. At the present time, humidification of the gases is the best way of controlling the water balance in the fuel cell. Therefore, the test apparatus should have the capability of fully humidifying both gases at the highest temperature and lowest pressure.

### 3.1.2 Control Requirements

As mentioned earlier, the test apparatus is designed to control the operating variables that have an impact on the performance of the fuel cell. Additionally, the test apparatus can make important decisions that cannot be made by the operator. Some of the controlling capability is automatic (set and controlled by the computer), and the operator sets the remaining controls. In general, those controls set by the operator are controlled with an instrument with the set point adjusted by the operator.

#### 3.1.2.1 Computer controls

Ideally, all parameters would be automatically controlled and adjusted through the computer interface, but this increases the complexity and cost of the test apparatus. Therefore, only certain variables were chosen for computer control. The mass flow of the inlet gases, the electronic load, and the temperature of the cooling water and water reservoir are all controlled automatically with set points adjusted through the computer interface.

#### 3.1.2.2 Manual controls

The gas temperatures, pressures, and humidity levels are adjusted directly by the

operator. The gas pressures, for instance, will be hand adjusted on the pressure regulators. The temperatures of the air and hydrogen will be controlled automatically, but the set points will be manually input to the heater control unit. Unlike some other variables, these variables do not require emergency computer adjustment.

#### 3.1.2.3 Safety overrides

Fuel cell systems require constant attention. Dangerous conditions can occur quickly that can affect the safety of the fuel cell and the operator. Certain well-established overrides have been laid out and must be included in the control strategy for the test apparatus. The most important override is an emergency kill switch that purges the fuel cell with nitrogen and disengages the load. This would be important in the event of a hydrogen leak. Additionally, for the protection of the fuel cell itself, the load must be disengaged if any of the cell voltages drop below a preset limit. This condition can happen quickly, so it must be monitored and acted upon by a computer.

## *3.2 System Designs*

With the design criteria determined, the detailed design of the fuel cell test apparatus can be accomplished. The design of each component is described in the following sections. While some of these components were designed up front and never adjusted, other component designs were revised or refined based on initial testing of the apparatus.

### 3.2.1 Fuel and Oxidant Gases

The fuel and oxidant conditioning systems are very similar in design. These systems are responsible for supplying the stack with the reactant gases (hydrogen and air) at the desired conditions. Generally, the gases are supplied to the stack through a series of components that regulate mass flow, pressure, temperature, and humidity level. The component designs are shown in detail in the following sections.

The connections between components for each system are made with 316 stainless steel tubing to reduce the number of cations transferred to the reactant gases. The inside diameter of the tubing affects the velocity and pressure drop in the system.

The velocity of each fluid depends directly on the tubing size and flow rate (determined previously). Assuming ideal gas behavior,

$$V_{gas} = \frac{\dot{m}_{gas}}{\frac{P_{gas}}{R_{gas} \cdot T_{gas}} \cdot A}, \tag{3}$$

where,

$\dot{m}_{gas}$ = the mass flow rate for each gas,

$P_{gas}$ = the lowest pressure for each gas,

$T_{gas}$ = the highest temperature for each gas,

$R_{gas}$ = the gas constant for each gas, and

$A$ = the cross sectional area of the tubing.

These velocities are used in the calculation of the pressure drop for each case. The pressure drop for turbulent flows depends on the gas density, viscosity, and velocity as well as the diameter of the tube. The following equation relates these quantities to the pressure drop per length of tube:

$$\frac{\Delta P}{Length} = 0.158 \cdot \rho_{gas}^{\ 0.75} \cdot \mu_{gas}^{\ 0.25} \cdot d^{-1.25} \cdot V^{1.75} \tag{4}$$

where,

$\rho_{gas}$ = the density of each gas,

$\mu_{gas}$ = the viscosity of each gas,

$d$ = the inside diameter of the tubing, and

$V$ = the velocity of each gas.

In order to reduce the noise created by the flow of gas through the tubing, the gas velocities were designed to stay below 25 m/s. Using this criteria, the fuel lines will use ½" tubing, and the air lines will use ¾" tubing. Additionally, this criteria corresponds to a pressure drop of less than 20 Pascals per meter for these tubing sizes, which is low enough to prevent pressure drop from having a significant effect on stack operation.

Although the line sizes are different, individual components comprising the two gas supply systems are essentially the same. The major differences are the supply and pressure regulation. The heating, humidification, and control of the mass flow rates are almost exactly alike. Each design is described in detail below.

#### 3.2.1.1 Mass Flow

As discussed in section 3.1.1.1, the maximum mass flows are determined by the maximum power and stoichiometry. The supplies of the two gases originate from different sources, but their control is the same. The oxidant, air, is supplied by a compressor. The air compressor must conform to strict standards in order to keep the air free of substances that could obstruct the membrane or destroy the catalyst. The compressor must be oil-free, and ideally, the wetted parts of the compressor would be manufactured of 316 stainless steel, but a compressor such as this would be unreasonably expensive. Therefore, the air is supplied by an oil-free air compressor with aluminum internal parts and a galvanized steel tank. It is assumed that the air in the tank is stagnant, and therefore, it will not carry any droplets water, which could contain the harmful cations, into the system. The hydrogen is supplied from compressed gas bottles. Although the bottles are carbon steel, there is little or no concern of picking up ions because the gas is dry.

Both fuel and oxidant gases are measured and controlled with programmable mass flow controllers. These devices are computer controlled. In order to provide sufficient measurement and control accuracy, two mass flow controllers are used for each gas system. A high range mass flow controller covers the entire range of mass flows for the specified system, but a low range controller will be used to measure and control mass

flows in the lower end of the high range controllers.

#### 3.2.1.2 Temperature

The temperature of the reactant gases entering the fuel cell must usually be greater than room temperature, but both the air compressor and hydrogen tank supply the gas at room temperature. The heating of the gases is accomplished with resistance heaters, but the methods are slightly different. This difference is a result of the flammability of diatomic hydrogen. While the air can be heated with a large heat flux produced by high heater surface temperatures, greater care must be taken to prevent the hydrogen from reaching its flammability limit (570°C). Therefore, the hydrogen must be heated at a lower heat flux. Unfortunately, pre-manufactured in-line gas heaters generally use large heat fluxes to shorten the heater length.

The amount of heat that is required to raise the gas temperature to a particular inlet temperature set point could be determined with a simple energy balance. However, the gases need to be heated well above the fuel cell inlet temperature to ensure that the temperature after humidification is approximately equal to the upper temperature limit. The total amount of energy that must be added to provide heating and humidification is determined in section 3.2.1.4

Additionally, low mass flow rates and high temperature differences require that the tubing be insulated. This is especially important due to the highly humidified gas. Cooling of either gas will cause condensation of the water vapor, and this condensation could quickly cause flooding of the fuel cell.

#### 3.2.1.3 Pressure

Due to the difference in gas supplies, the pressure regulation will also be slightly different. Additionally, the fact that the hydrogen is run dead-ended, while the air is in an open system, will change the pressure regulation schemes. The regulation of the hydrogen pressure, which is shown in Figure 3-1, will be as simple as changing the pressure setting on the regulators. Adjustment of the filter regulator changes the pressure at (1), and the pressure at the inlet of the fuel cell (2) depends on the pressure drop through the system. In this scheme, the mass flow controller does not control the flow of

hydrogen as long its set point is greater than the amount of fuel the stack is using.

The air, because it is run open-ended, will require a backpressure regulator. The back-pressure regulator controls the pressure at point (2) in Figure 3-2, and a filter regulator positioned before the mass flow controller will set point (1) to a higher pressure according to the pressure drop of the entire system. A schematic of the air pressure regulating system is shown in Figure 3-2 below:

The air in the compressor tank varies in pressure depending on the amount of air used since the last compressor cycle, but the first pressure regulator keeps the system pressure downstream (1) steady with changes in tank pressure. The pressure of the fuel cell inlet gas will be equal to the pressure just before the backpressure regulator (2) plus any pressure drop through the fuel cell. Likewise, the pressure just downstream of the mass flow controller is the pressure at the inlet of the fuel cell plus any pressure drop between there and the mass flow controller. The mass flow controller creates a pressure drop itself in order to control the amount of mass flowing through the system. The mass flow controller will adjust the orifice size in order to produce the desired mass flow.

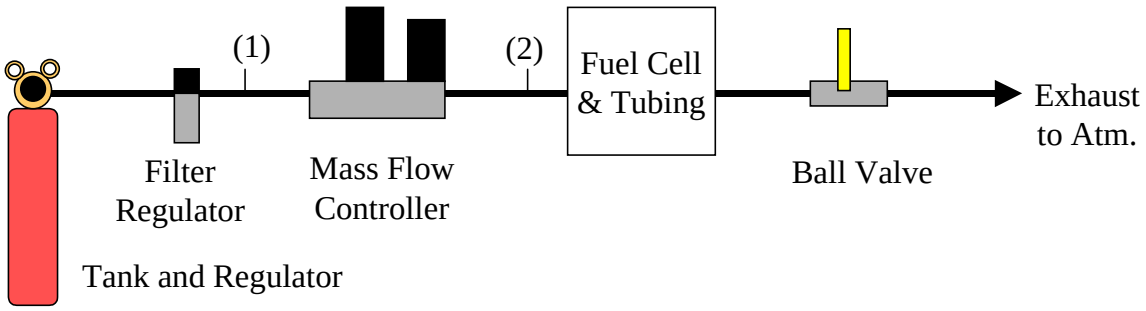


**Figure 3-1. Hydrogen pressure regulation schematic**

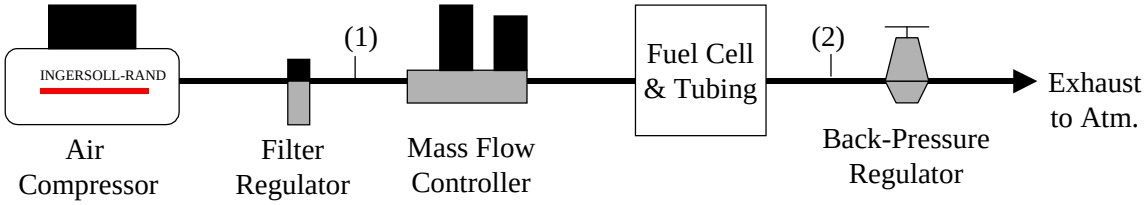


**Figure 3-2. Air pressure regulation schematic**

### 3.2.1.4 Humidity

Humidification of gas streams to near saturation is a difficult process, especially at higher temperatures. The prototype test apparatus will spray water into the previously heated gas to provide humidification. The following calculation shows the ideal amount of water needed to humidify air to the desired relative humidity and outlet temperature. The amount of water required for humidification is based on the mass flow of the air and the specified inlet conditions:

$$\dot{m}_w = \dot{m}_{gas}(\omega_{fci} - \omega_o) \tag{5}$$

where,

$\dot{m}_{gas}$ = the mass flow rate of each gas,

$\omega_o$ = the source gas humidity ratio, and

$\omega$ = the design humidity ratio of each gas at the inlet to the fuel cell.

The humidity ratio, $\omega$, is given by:

$$\omega = \frac{M_{wr}}{M_{gas}} * \frac{\Phi * p_{sat}(T_{out})}{P - \Phi * p_{sat}(T_{out})}\ , \tag{6}$$

where,

$P$ = the design pressure,

$p_{sat}$ = the saturation pressure at the temperature, $T_{out}$,

$T_{out}$ = the temperature of the gas at the inlet to the fuel cell, and

$\Phi$ = the relative humidity of the gas.

Therefore, the humidity ratio and the amount of water required for humidification can be determined knowing the temperature, pressure, and the relative humidity of both the inlet and outlet gases. The volumetric flow of humidification water for each gas stream is found by combining equations (5) and (6) and introducing the density of water:

$$\frac{\dot{V}_w}{\dot{m}_{gas}} = \frac{1}{\rho_w}\frac{M_w}{M_{gas}}\left(\frac{\Phi_{fci} * p_{sat}(T_{fci})}{(P_{fci} - \Phi_{fci} * p_{sat}(T_{fci}))} - \frac{\Phi_o * p_{sat}(T_o)}{(P_o - \Phi_o * p_{sat}(T_o))}\right) \quad (7)$$

where,

$\rho_w$ = the density of water (1000 kg/m$^3$),

$M_w$ = the molar weight of water (18.02 g/gmol),

$M_{gas}$ = the molar weight of each gas,

$\Phi_{fci}$ = the relative humidity at the fuel cell inlet,

$T_{fci}$ = the temperature of each gas at the fuel cell inlet,

$P_{fci}$ = the pressure of each gas at the fuel cell inlet,

$\Phi_o$ = the relative humidity of the source gas,

$T_o$ = the temperature of the source gas, and

$P_o$ = the pressure of the source gas.

The water required to humidify the air stream is based on the humidity ratio of saturated air at the source, which corresponds to the temperature and pressure in the tank (25°C, 690 kPa gauge). Determination of the water needed to humidify the hydrogen stream is similar, except the initial humidity ratio is assumed to be zero, or completely dry. The plots in Figure 3-3 show the milliliters of water per standard liter of gas needed to humidify the gases to the desired relative humidity and temperature. As expected, the amount of humidification water increases with outlet temperature and relative humidity.

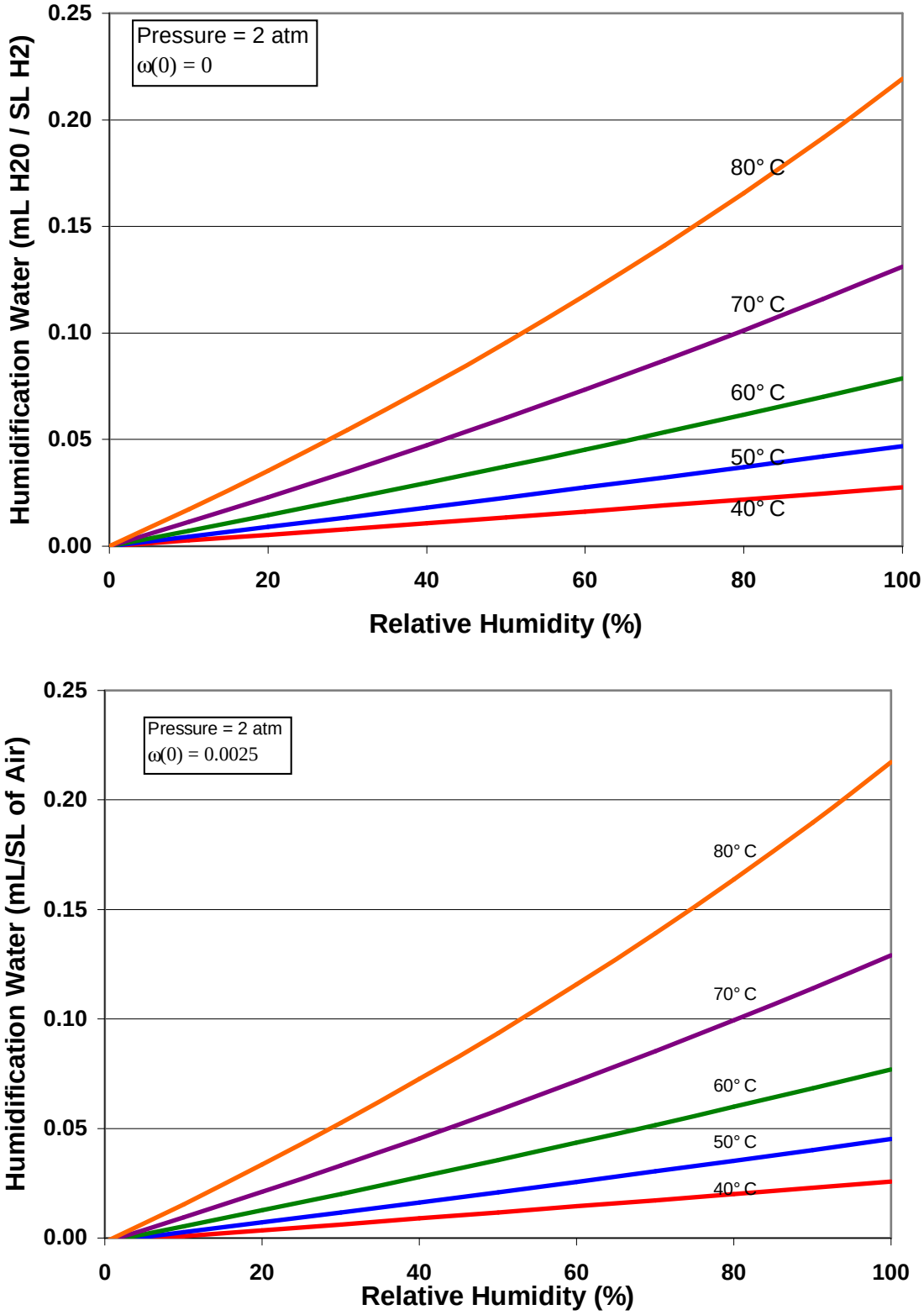


**Figure 3-3. Humidification water vs. relative humidity and fuel cell outlet temperature**

The plots also indicate that as the temperature rises, the necessary water increases by a great deal, especially at higher humidity levels. For example, at 90 percent relative humidity almost ten times as much water is needed if the outlet temperature is doubled from 40°C to 80°C.

The amount of water required to humidify the two gas streams is practically the same on a mass flow basis. This results from the definition of the relative humidity. The relative humidity of a gas depends on the vapor pressure, which is related to the mole fraction of water in the mixture, and the saturation pressure, which depends on the gas temperature. Therefore, the water required to humidify a unit of mass of the two gases to the same temperature and relative humidity would be identical if each started completely dry, but there is a slight difference due to the initial amount of water in the air. Of course, the actual amount of water needed for each gas stream is drastically different due to the large difference in mass flows rates of the two gases.

The flow of humidification water is supplied by a deionization bed connected to a city water source and is controlled with small valve-adjusted flow meters. The actual flow rates for the humidification water need to be much higher than the calculated value because a large portion of the water will be sprayed onto the tubing walls. For this reason, drain traps must be installed downstream of the spray nozzles to dispose of any excess water. Also, any large droplets of water in the gas streams must be knocked out to prevent them from flowing into the fuel cell and possibly flooding it. This is accomplished with an open space of significantly larger diameter in order to slow the velocity of the gas and remove the droplets.

The vaporization of this amount of water requires a large amount of energy, which is called the enthalpy of vaporization. Normally, this energy would be provided by the gas, decreasing its temperature. In order to yield humidified hydrogen and air at the specified fuel cell inlet temperature, a heater will add energy to the humidification process. The necessary heat to be added is calculated using the conservation of energy. Assuming the air and hydrogen are ideal gases, the amount of heat necessary to achieve the desired relative humidity and outlet temperature is determined by:

$$\frac{\dot{Q}}{\dot{m}_{gas}} = \left(h_{gas}\left(T_{fci}\right) + \omega_{fci} \cdot h_{w,g}\left(T_{fci}\right)\right) - \left(h_{gas}\left(T_o\right) + \omega_o \cdot h_{o,g}\left(T_o\right)\right) - \left(\omega_{fci} - \omega_o\right) \cdot h_{w,f}\,, \qquad (8)$$

where,

$h_{gas}\left(T_{fci}\right)$= the enthalpy of each gas at $T_{fci}$, the temperature of the gas at the inlet to the fuel cell,

$\omega_{fci}$ = the humidity ratio at the inlet to the fuel cell,

$h_{w,g}\left(T_{fci}\right)$= the enthalpy water vapor at $T_{fci}$, the temperature of the gas at the inlet to the fuel cell,

$h_{gas}\left(T_o\right)$= the enthalpy of each gas at $T_o$, the temperature of the source gas,

$\omega_o$ = the humidity ratio of the source gas,

$h_{w,g}\left(T_o\right)$= the enthalpy water vapor at $T_p$, the temperature of the source gas, and

$h_{w,f}\left(T_{amb}\right)$ = the enthalpy of liquid water at $T_{amb}$, the ambient temperature.

The plots in Figure 3-4 show the amount of energy per standard liter of gas that must be added to humidify each gas to the specified RH and temperature. As expected, it requires a great deal of energy to heat and humidify the inlet streams, especially to the higher temperature and humidity levels. Similar to the plots showing the required amount of water for humidification, the amount of additional energy required to humidify a unit of mass of each of the two gases is essentially the same. Because the two gases require approximately the same amount of water for humidification, the specific energy required to humidify the gases is also approximately equal. Similar to the required humidification water, the actual heat required differs between the two gas streams because of the difference in their mass flow rates.

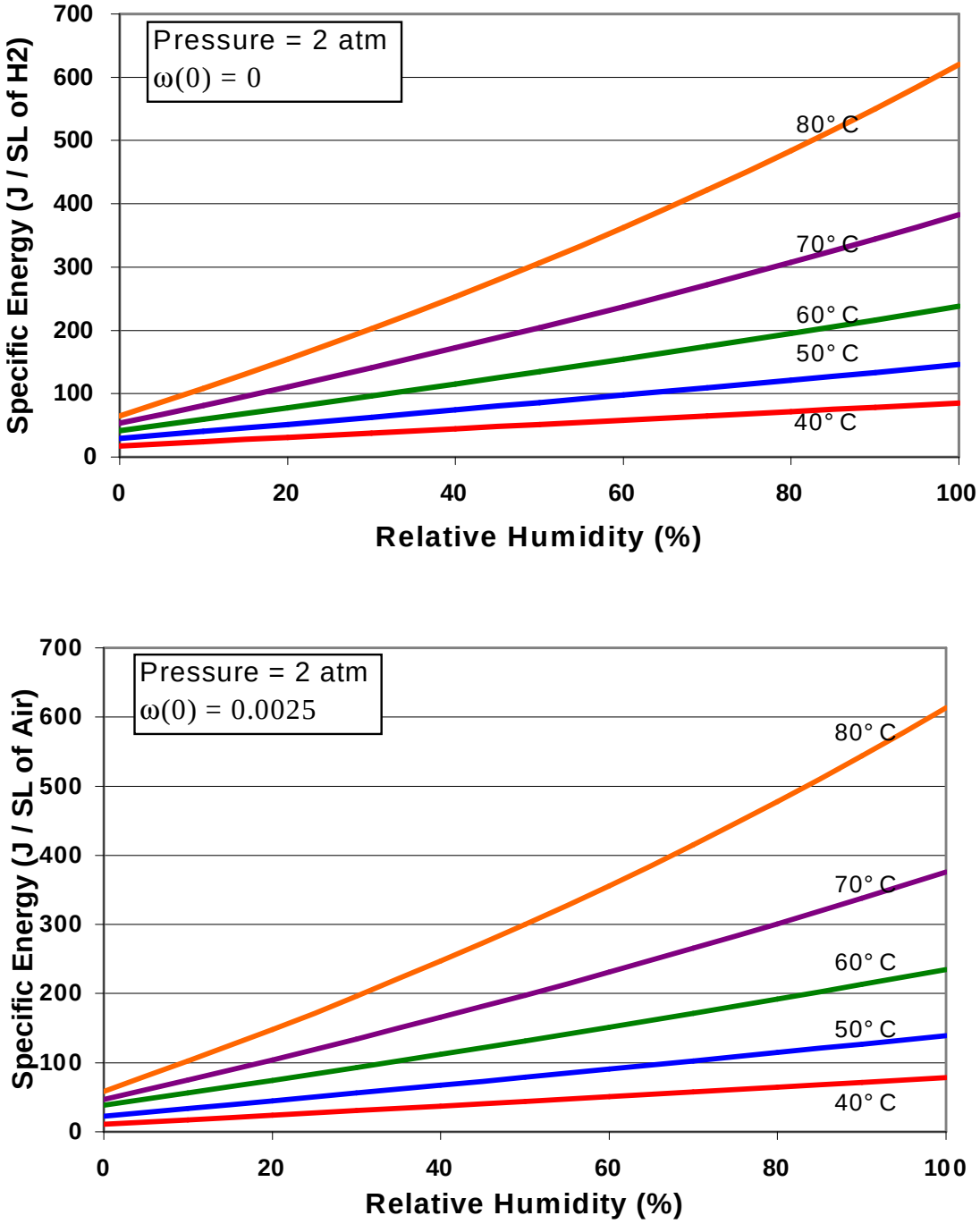


**Figure 3-4. Humidification energy vs. relative humidity and fuel cell outlet temperature**

### 3.2.2 Coolant Water

The coolant water is an extremely important system in the fuel cell test apparatus. With an overall efficiency near 50 percent, fuel cells yield approximately as much heat as

they do electricity, and coolant water is required to transfer the heat from the fuel cell. Also, the coolant water is primarily responsible for keeping the fuel cell at a constant temperature, which increases the efficiency of the stack. The water, however, must be very pure in order to prevent electricity from flowing through it.

#### 3.2.2.1 Flow

The cooling water is stored in a large tank, which is sized according to its thermal capacity. The tank, or reservoir, will have the thermal capacity for five minutes of heat removal from the stack at its maximum thermal power output. The tank volume calculation is shown below:

$$V_{reservoir} = \frac{\Delta t \cdot \dot{Q}}{\rho_w \cdot c_{p,w} \cdot \Delta T} \tag{9}$$

where,

$\Delta t$ = the amount of elapsed time (300 seconds),

$\dot{Q}$ = the maximum amount of heat generated by the fuel cell (10 kW),

$\rho_w$ = the density of water (1000 kg/m$^3$),

$c_{p,w}$ = the specific heat of water (4184 J/kg K), and

$\Delta T$ = the allowable temperature rise (10 K).

Using these values, the reservoir volume was determined to be 72 liters. The water is circulated through the stack by a pump. The maximum flow rate is determined by the amount of heat that must be removed from the fuel cell The maximum flow rate was designed to remove 10 kW, which is twice the maximum electrical power, at a ten degree temperature rise. The calculation is shown below.

$$\dot{V}_{cw} = \frac{\dot{Q}}{\rho_{H_2O} \cdot c_p \cdot \Delta T} \tag{10}$$

where,

$\dot{Q}$ = the maximum amount of heat generated by the fuel cell (10 kW),

$\rho_w$ = the density of water (1000 kg/m$^3$),

$c_{p,w}$ = the specific heat of water (4184 J/kg K), and

$\Delta T$ = the allowable temperature rise (10 K).

The maximum flow rate of coolant water, using the values above, is 18 LPM. Since the pump runs at a single speed, a three-way valve that directs the coolant water either to the fuel cell or back into the reservoir will control the flow rate. This valve can be adjusted to guide more or less water to the fuel cell. The pump must have 316 stainless steel or better wetted parts to maintain the purity of the water.

#### 3.2.2.2 Temperature

An immersion heater in the storage tank will heat the circulating water in order to keep the water at the desired temperature during start-up. The heater is designed to heat the tank of water from 21°C to 60°C in one hour. The storage tank temperature will be controlled by a combination of a high-limit controller and the measurement and control program. A definite-purpose contactor will be placed in the power line to the immersion heater. The computer program will choose to open or close the contactor depending on the temperature of the reservoir. The control program will use a simple on/off control with a deadband to keep the tank temperature at the set level. The high-limit controller will have the capability to break the circuit for the contactor, if the tank temperature rises above the high-limit set point.

While the water is initially heated in the reservoir, during operation, the temperature of the coolant at the inlet to the fuel cell must be controlled to keep the stack at a constant temperature. To control the temperature of the fuel cell, the coolant water flows through a heat exchanger. Cold city water flows counterflow through the other side of the heat exchanger. The flow rate of city water through the heat exchanger is

varied to adjust the temperature of the coolant water. This flow rate is adjusted with an electronically actuated globe valve placed at the drain. Opening the valve increases the heat transfer and lowers the coolant water temperature, and closing the valve raises the circulating water temperature.

#### 3.2.2.3 Purity

For many stack designs, the coolant water is in direct contact with the electrically conductive components. Thus, the resistivity of the coolant water must be maintained and monitored. A resistivity sensor is mounted in the water line to measure the purity of the water. The coolant water should not have a resistivity of less than 2 MΩ-cm. This level of purity will be maintained with a clean system at start-up and an in-line deionizing bed. An additional deionizing bed provides a supply of purified water for filling the tank, cleaning parts, etc.

### 3.2.3 Load

The electric load is the driving force for the entire fuel cell and, therefore, for the test apparatus. Applying a load to the fuel cell at the wrong time can cause serious damage to the device. Because of this, the load applied to the stack must be programmable and must have the capability of disengaging quickly under the control of a computer.

Fuel cells are low voltage and high current devices, and the electric load must have the capability to measure and draw loads such as this. The test apparatus is designed to investigate low power fuel cells, which means that the voltage across the stack may only be 2-3 volts while the current is as high as 500 amps.

### 3.2.4 Measurement/Control

Finally, the test apparatus will have the ability to record data, control components, and make critical decisions. This will be accomplished with a computer controlled data acquisition and control system. The system must to be able to monitor critical values faster than twice a second and make decisions according to the measurements. It will also have the capability to adjust set points of certain control devices by varying their

signal voltages.  Additionally, the measurement and control program will need to display all the important data during testing.

# 4 TEST APPARATUS CONSTRUCTION

The test apparatus was constructed to meet the design criteria set forth in the previous chapter. As construction progressed, systems were evaluated and revised as necessary to provide the required performance.

## *4.1 Basic Materials*

All of the connections between components use 316 stainless steel tubing. Great care was taken to ensure that the system was clean when assembled. All of the tubing was cleaned with isopropyl alcohol, flushed with deionized water, and blown out with nitrogen. The tubing was cut with a tube cutter, and any burrs remaining were removed before assembly.

Stainless steel compression fittings are used in every possible tubing connection. All other connections are threaded pipe fittings. Gas line or military grade Teflon tape is used in all threaded pipe fittings. Teflon tape should always be used on every 316 stainless steel connection to prevent gauling of threads. Turns in the tubing lines were bent where possible. Bending the tubing reduced the pressure drop and lowered fitting costs as well as reducing the opportunity for leaks. Some tight turns could not be accomplished with the tubing bender, and compression tubing elbows were used.

All low voltage wiring (less than 120 VAC) except thermocouples uses two-conductor, shielded, 22 gauge wire with a ground wire. Thermocouples use 24 gauge type T thermocouple wire. Power wiring for 120 VAC circuits use rubber jacketed copper wire greater than 18 gauge. High current and low voltage connections to the fuel cell use 1/0 gauge wire or greater in order to reduce Ohmic resistance.

## *4.2 Layout*

The test apparatus consists of a display board, a water system module, a heating and humidifying module, and a data acquisition cabinet. Appendix 2 shows a plan view of the test apparatus bay in the Ware Lab, and Figure 4-1 shows a schematic of the entire test apparatus. The majority of components are attached to the display board to ease

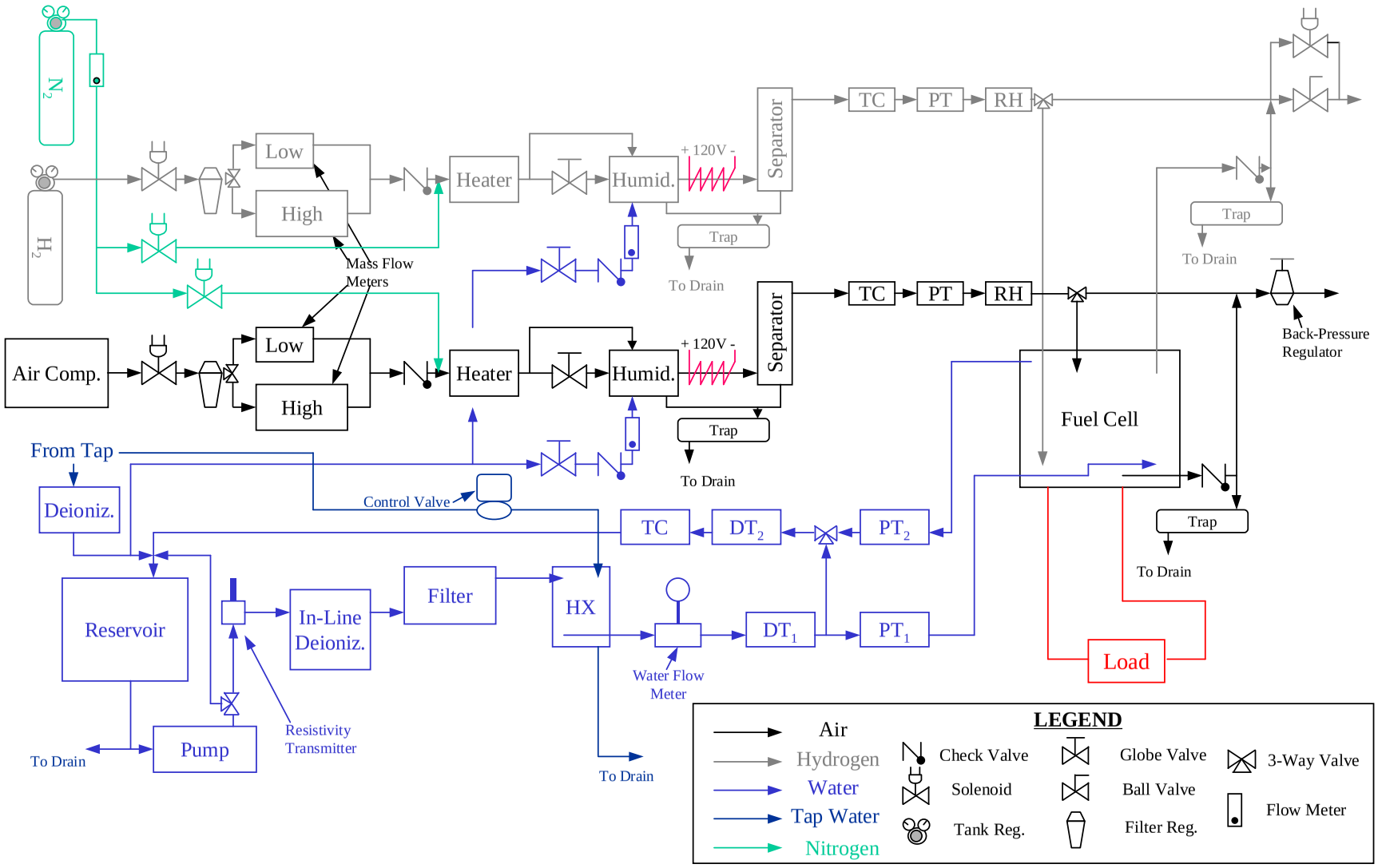


**Figure 4-1. Process Schematic for PEM Test Apparatus**

explanation and demonstration of the test apparatus. The water module needed to be adjacent to the display board due to the large size of the reservoir tank. The air and hydrogen heaters are placed on a small stand directly in front of the display board, and the computer, data acquisition mainframe, and electric load are placed in a moveable cabinet with locking doors for security purposes.

### 4.2.1 Fuel

The fuel system is primarily located on the display board flowing from left to right. The hydrogen bottle, which is assigned part number H-1 referencing Figure 3 in Appendix 2, is positioned at the leftmost part of the display board. Hydrogen flows through the primary pressure regulator (H-2) directly out of the bottle. Next, a normally closed solenoid valve (H-3) prevents the flow of hydrogen if the emergency switch is depressed. This design requires electrical current through the solenoid to allow the flow of hydrogen. After the solenoid, the secondary regulator (H-4), which includes a filter as well, is used to control the final pressure in the fuel line. The hydrogen then travels through one of two mass flow controllers. One of the mass flow controllers (H-6) is used for mass flow rates of hydrogen greater than 40 SLPM, and the other (H-7) controls mass flow rates between 0.8 and 40 SLPM. A 316 SS three-way valve (H-5) allows the operator to choose which controller to use depending on the desired mass flow rate. The mass flow controllers will measure the hydrogen flow and report it to the data acquisition system and control the hydrogen flow in response to a signal from the data acquisition system.

Following the mass flow controllers, a check valve (H-8) prevents back flow of gas into the mass flow controllers for any reason. The hydrogen flows to the heating and humidification module where it is heated in a long piece of tubing wrapped with a rope heater (H-9). The temperature of the heated hydrogen is measured with a thermocouple (H-10). The Eurotherm heater control unit adjusts the heater power according to this temperature. After the heater and thermocouple, the gas flow splits. A small portion of the flow is used to atomize water in the spray nozzle (H-12c) located in the spray chamber (H-12). The remaining flow enters the spray chamber itself. A globe valve (H-11) after the flow separation is used to balance the flow between the atomizing line and

the main flow. The globe valve is adjusted to attain the desired pressure difference between the main flow and nozzle flow. The small amount of flow entering the spray nozzle is, therefore, at a higher pressure, which creates a finer atomization of water for humidification. Both of these lines are connected to a pressure gauge (H-17) with a three-way valve (H-16) to measure the pressure of either flow on the same gauge.

From the spray chamber, a fine mist of water is sprayed downstream with the hydrogen in order to increase its humidity level. This water is supplied from a deionizing bed at the water module. Before entering the nozzle, the water must flow through a ball valve (H-13) and a check valve (H-14). Then, a flow meter (H-15) with a flow control valve controls the volume of water entering the humidifier. After the water is sprayed into the hydrogen, the hydrogen and water mix humidifying the gas, while a rope heater (H-19) adds heat to the process. Next, the mixture enters a separation chamber (H-20) of significantly greater diameter. The flow velocity is reduced, and any droplets of water are removed from the gas stream. Any separated liquid water flows into a drain trap (H-18) located below the separation chamber. The spray chamber also has a drain connection that enters the same trap.

Finally, the hydrogen flows past a thermocouple (H-21), pressure transducer (H-22), and relative humidity sensor (H-23) just before entering the fuel cell (H-25). However, the gas flow can also be directed around the fuel cell. An operator controlled three-way valve (H-24) guides the gas stream through or around the fuel cell. This allows the hydrogen to reach the proper conditions before being directed into the stack.

At the outlet to the fuel cell (H-26), a check valve (H-27) prevents unintentional backflow into the stack. During a test, the fuel cell exit gas stream is stopped by a ball valve (H-31). Another drain trap (H-29), which has a vent (H-30) connected to the fuel cell bypass, is located after the fuel cell to collect any liquid water. Also, a normally open solenoid valve (H-28) is placed after the fuel cell to release the hydrogen to the atmosphere in case of an emergency. The hydrogen line is exhausted to the roof of the building through an additional ball valve (H-32). A flame arrestor (H-33) is placed at the exhaust point to prevent any flames from traveling backwards through the exhaust should

there be an ignition at the outlet.

### 4.2.2 Oxidant

The oxidant system layout, which is shown in Figure 4 of Appendix 2, is very similar to the fuel system. Whereas the fuel system starts with the hydrogen tank, the oxidant system originates at the air compressor (A-1), which is located in the back left corner of the Ware Lab bay. A length of 316 stainless steel pipe brings the air from the compressor to the left side of the display board. Similar to the hydrogen, a normally-closed solenoid valve (A-2) is placed just before the air filter regulator (A-3). This solenoid valve closes to automatically engage the purge system in emergency situations. The pressure regulator keeps the air pressure in the fuel cell constant while the compressor tank varies in pressure. The operator directs the air to either the high (A-5) or low (A-6) range mass flow controller with a 3-way valve (A-4). The mass flow controller, which communicates with the data acquisition system, makes measurements and adjusts a valve to control the amount of airflow.

After the mass flow controller, the air passes through a check valve (A-7) and proceeds to the heating and humidification module. The flow path of the air is similar to that of the hydrogen, but one difference occurs just before the heater. The Omega in-line air heater (A-8) cannot handle the maximum flow rate of air, so a bypass line with a globe valve (A-9) adjusts the amount of air flowing through the heater. Similar to the hydrogen system, a thermocouple (A-10) measures the heater outlet temperature and relays it to the Eurotherm controller. The air flows from the heater or bypass and is split exactly like the hydrogen in order to provide hot air to the spray nozzle (A-12c). A globe valve (A-11) adjusts the amount of air flowing through or around the spray nozzle by reducing the pressure of the air flowing around the spray nozzle. Again, the pressure difference is used to create a fine atomization of water for humidification. As in the hydrogen system, a pressure gauge (A-17) with a 3-way valve (A-16) measures that pressure difference.

The air then flows through the spray chamber (A-12), and the humidification water is sprayed into the hot air. The humidification water originates from the same

source as the humidification water for the hydrogen, and just like the hydrogen, the water flows through a ball valve (A-13), a check valve (A-14), and a water flow meter (A-15), which has a valve to control the flow rate. In the gas stream, another rope heater (A-19), which is identical to those used on the fuel system (H-9 and H-19), is used to add heat to the humidification process in the length of tube between the spray chamber and the separator. The hot mixture flows into the water separator (A-20) where the water droplets in the air separate from the humid air. The liquid water is collected in a drain trap (A-18) exactly like those used in the hydrogen system. The drain trap is located below the separator, and it removes water from both the spray chamber and the water separator.

Next, the hot, humid air flows toward the fuel cell inlet (A-25), but just before it arrives, the measurement and control program reads the temperature (A-21), pressure (A-22), and relative humidity (A-23). Similar to the hydrogen system, the air can be bypassed around the fuel cell by changing the position of a three-way valve (A-24). The bypass connects to the fuel cell outlet (A-26), where a check valve (A-27) prevents any reverse flow to the stack. In either mode (bypass or fuel cell), any liquid water in the flow is collected in a trap (A-29) and drained. The trap vent (A-30) connects to the exhaust just before the backpressure regulator (A-28). The backpressure regulator is a spring-loaded valve that keeps the upstream gas pressure at the desired level. Turning a knob, which compresses or decompresses the spring, adjusts the pressure setting. A ball valve (A-31) is located in the tubing that leads to the roof where it is exhausted to the atmosphere.

### 4.2.3 Coolant

Figures 5 and 7 in Appendix 2 detail the coolant water system, which includes components on the display board and the water module. The module consists of a reservoir, pump, two deionizing chambers, filter housing, heat exchanger, flow meter, backflow preventer, and a flow control valve. The heated, deionized water is stored in the reservoir (C-1) until drawn out by the pump (C-3) or flushed to the drain by opening a ball valve (C-2). While in the tank, the water is heated by an immersion heater (C-1b). A thermocouple (C-1c) measures the reservoir water temperature, and a level switch (C-

1a) tells the control program if the tank has an acceptable amount of water. The water discharged from the pump can be directed through the coolant line or to the reservoir return (C-5) by a three-way valve (C-4). The resistivity of the line water is measured (C-6) before it flows through an in-line deionizing bed (C-7) and filter (C-8). After the filter, the water flows into the plate heat exchanger (C-9) where cold city water cools the coolant to the temperature required to maintain the fuel cell outlet temperature. An electrically actuated valve (C-10) adjusts the cold water flow rate.

After the heat exchanger, the water flow rate is measured by a turbine flow meter (C-11) and flows into a long run of tubing towards the display board and fuel cell. Before the water enters the fuel cell, the data acquisition system records its pressure (C-13) and a thermocouple (C-12a) reads the inlet temperature for the differential temperature meter (C-12), which transmits the temperature difference between the inlet and outlet to the data acquisition unit. The coolant receives heat as it circulates through the fuel cell, and, after exiting the stack, the outlet pressure reading is taken as well as two temperature measurements. The first thermocouple (C-18) sends the outlet temperature to the control program, and the second thermocouple (C-12b) is used by the differential temperature meter. The operator may turn a three-way valve (C-17) to bypass the water around the fuel cell during the coolant water system start-up. Finally, the water returns through a long length of tubing to the reservoir.

### 4.2.4 Load

The electrical load is located directly to the right of the display board in the data acquisition cabinet. Large 1/0 gauge wire connects the load to the bus plates of the fuel cell. The computer program controls the load setting, and two safeties are present to ensure that the operator and fuel cell stay clear of danger. First, the load setting is connected to a normally open relay, which loses power when the emergency switch is tripped. Also, the computer program monitors the cell voltages of the fuel cell and can switch off the load when one falls below a safe limit.

### 4.2.5 Measurement/Control

A LabVIEW program governs the measurement and control routines. The

program communicates with a separate HP data acquisition unit and an analog output voltage card in the PC to read and control all of the devices. A wiring schematic is shown in the Figure 4-2 below. The very first priority of the program is to monitor the individual cell voltages of the stack. It reads these voltages every 0.5 seconds and makes a decision based on the result. If any of the voltages is less than 0.4 volts, the switch through which the load signal passes is disengaged removing the load.

The next priority is given to reading the measurement instruments throughout the system. Due to the slow nature of the communication between the LabVIEW program and the HP data acquisition system, the instrument readings are taken two channels at a time along with the cell voltages. A complete set of readings is taken approximately every five seconds. In this five second period of time, the cell voltages are monitored a total of nine times. The instrument values are then displayed on the panel and in graphs for each of the different systems. Finally, the operator can prompt the program to make changes to the control settings.

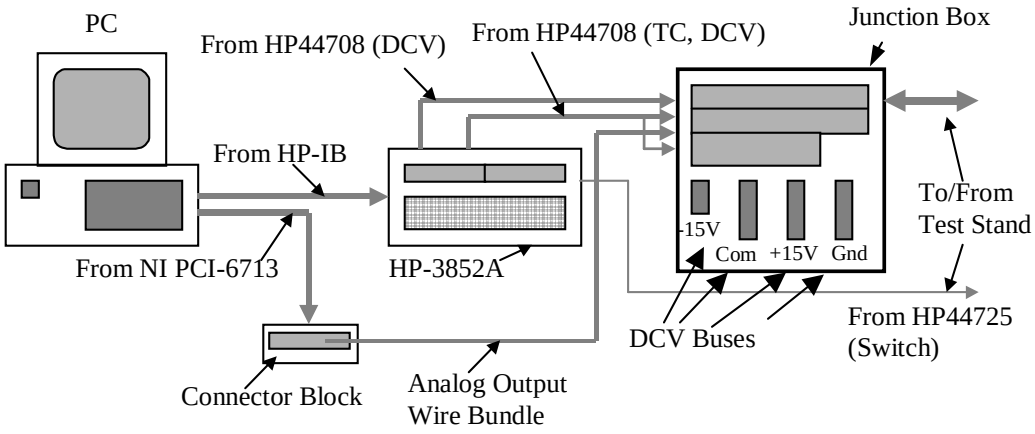


**Figure 4-2. Measurement / Control Wiring Schematic**

## *4.3 Assembly*

The initial implementation of the fuel cell test apparatus differed slightly from the original design. Problems were found with a few selected components, and temporary design adjustments were made. First, the turbine flow meter in the coolant system stopped responding. It was replaced with a variable area water flow meter just before the

resistivity transmitter (C-6 in Appendix 2 figure 8). The temporary flow meter was used to develop a relationship between the coolant pressure drop and flow rate for the fuel cell. During a test, the flow meter was replaced with a length of 316 stainless steel tubing, and the pressure drop was used to determine the coolant flow through the stack.

Additionally, the electrically actuated control valve (C-10 in Appendix 2 figure 8) that adjusted the city water flow through the heat exchanger repeatedly malfunctioned. Therefore, a globe valve was placed at the drain of the cold water loop in the heat exchanger. The valve was manually adjusted to set the fuel cell outlet temperature of the coolant to the desired value.

The following sections describe in detail the individual components used in the original design of the test apparatus and in the initial implementation.

### 4.3.1 Fuel and Oxidant

The gas delivery systems are constructed with the components specified in the following sections. The part numbers listed correspond to those in Appendix 2. First, any devices common to both the air and hydrogen systems are described. Then components unique to each system are discussed.

#### 4.3.1.1 Common Devices

Mass Flow Controllers (H-6, H-7, A-5, and A-6)

Sierra Side-Trak model 840 mass flow controllers are used to control and measure the flow of hydrogen and air through the system. The electrical connections for the Sierra mass flow controllers are made with an included card connector on top of each controller. Each device requires a +15 VSC and –15 VDC power supply, a 0-5 V input signal, and a 0-5 V output signal connection. The input and output signals are proportional to the maximum mass flow rates of the valves.

**Table 4-1 Specifications for Sierra mass flow controllers**

| System | Range | Mass Flow Range (SLPM) | Accuracy (SLPM) | Tube Connections |
|---|---|---|---|---|
| Hydrogen | Low | 0-40 | +/- 0.4 | 1/4” |
| Hydrogen | High | 0-170 | +/- 1.7 | 1/2” |
| Air | Low | 0-100 | +/- 1.0 | 3/8” |
| Air | High | 0-500 | +/- 5.0 | 1/2” |

Table 4-1 shows the mass flow ranges, accuracy, and the connections for each of the controllers. The accuracy is ± 1 percent of the full-scale mass flow for each controller.

The electrical connections for the Sierra mass flow controllers are made with an included card connector on top of each controller. Each device requires a +15 VDC and –15 VDC power supply, a 0-5 V input signal, and a 0-5 V output signal connection. The input and output signals are proportional to the maximum flow rates of the valve.

Filter Regulator (H-4 and A-3)

Both gas systems use Watts stacked filter regulators to control line pressure and eliminate droplets of water from the flow. Water droplets must be removed from the gas streams before entering the mass flow controllers. These filter regulators are constructed of 316 stainless steel and are capable of regulating pressures up to 125 psig. The outlet pressure is adjustable by a knob atop the device, which can be locked in position. The regulators have three ¼” NPT outlets. One outlet is used to transfer the regulated gas to the system, and one of the outlets leads to a 0-150 psig pressure gauge made from 316 stainless steel.

Humidifier (H-12 and A-12)

Gas stream humidification uses a Bete spray nozzle in a manufactured housing to inject atomized water into the gas. Greater atomization of the water can be achieved by flowing

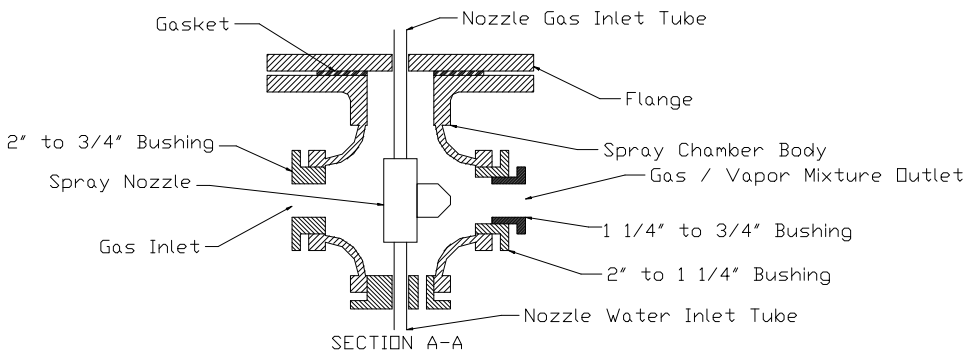


**Figure 4-3. Spray chamber schematic**

hydrogen or air, which must be at a higher pressure than the line gas stream, through the nozzle as well. The nozzle is positioned inside a 2" 316 stainless steel cross, which is shown in Figure 4-3. A flange is welded to the top port of the cross, and feet

were attached to the bottom port. The unhumidified gas enters from one of the side ports where it flows over the spray nozzle and is injected with atomized water. Leaving the spray chamber, the mixture travels through a short section of ¾" tubing (approximately 2 feet) where it enters the separation chamber. A 60 inch, 250 Watt rope heater is wrapped around the spray chamber and short length of tubing in order to provide heat for vaporization.

The separation chamber is a 316 stainless steel double filter housing. It measures 3 ½" in diameter and approximately 22" in height. The separated liquid water drains through a tube attached to the bottom of the chamber that leads to the drain trap.

Drain Trap (H-18, H-29, A-18, and A-29)

The four drain traps in the fuel and oxidant systems are manufactured from 316 stainless steel 1 ½" pipe (Figure 4-4). One trap is located on the heating and humidifying module for each humidification process (two traps total), and the remaining two traps drain any liquid water from each gas stream at the exit of the fuel cell.

The traps operate with the use of a solenoid valve controlled by a level switch. The excess water collects in the pipe, which lays horizontal with two rounded end caps butt welded to the ends. Water drains into the side of the trap via a ½" threaded coupling

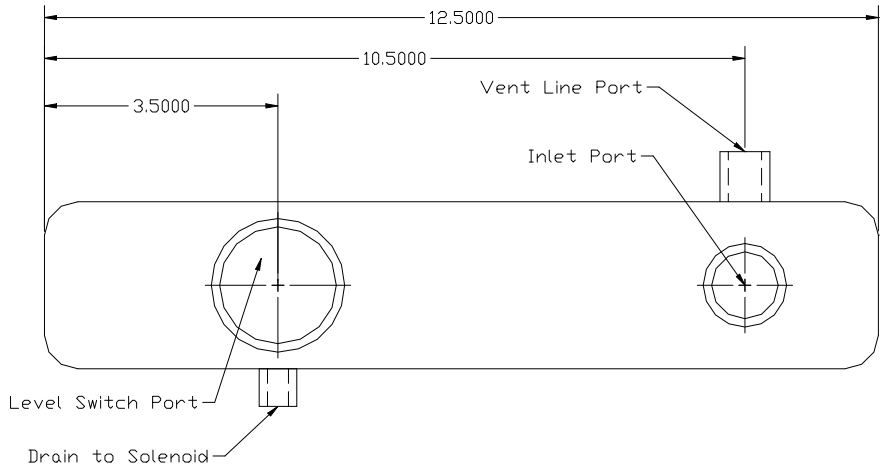


**Figure 4-4. Drain trap schematic**

welded to the trap. The level switch also screws into a 1" threaded coupling welded on side of the pipe. The level switch is constructed mostly from stainless steel (most likely not 316), but the float is made from polypropylene. A 1/8" coupling is welded on the bottom of the pipe, to which the solenoid is connected. The solenoid switch is normally closed with 1/8" NPT connections. The body is manufactured from 316 stainless steel. The water leaving the solenoid valve travels through a rubber hose to a hub drain in the lab. Finally, one ¼" threaded coupling is attached to the top of the pipe. This final connection allows the gas in the trap to escape if a slug of water blocks the drain line. Without the vent line, gas stuck in the trap could prevent any additional water from entering the trap, which would cause flooding in the system the trap is designed to drain. The vent is attached downstream of the drain connection. Therefore, any gas that needs to escape is pushed to a location in the system with a lower pressure.

Heater Control Unit

Eurotherm model 810 temperature controllers regulate both the air and the hydrogen heaters. The controllers monitor a type T thermocouple and adjust the duty cycle to a 120 VAC heater in order to bring the heater outlet temperature to the desired set point. The controllers use a continuous PID control routine, which was tuned using Eurotherm's instructions. The set point is adjustable with pushbuttons on the controller,

and it has an accuracy of ± 0.25 percent of the span of the controller.

#### 4.3.1.2 Fuel System Components

Because of the nature of hydrogen, the fuel system uses different components for certain sub-systems. The part numbers mentioned in each description match those used on the system diagram in Appendix 2 figures 3 and 6.

Regulator (H-2)

A Concoa pressure regulator controls the hydrogen pressure leaving the bottle. The regulator type is CGA type 350 rated for hydrogen use, and it is constructed of brass. Stainless steel was not used since the gas leaving the hydrogen bottle is extremely dry. It has an inlet pressure rating of 4000 psi, and an outlet pressure limit of 150 psi. The regulator is manually controlled with a knob and has inlet and outlet gauges.

Heater (H-9)

The hydrogen heater was constructed from ½" 316 stainless steel tubing and one 60" 250W rope heater. A 50" piece of tubing is bent 180° in two places, which allowed for a more compact heater. The rope heater wraps around the tubing approximately once per two inches of tubing length. It was secured with a piece of high temperature foil tape (rated for 320°C). In order to ensure that the majority of heat is transferred into the hydrogen, a 24" piece of galvanized steel duct surrounds the heater assembly, and fiberglass is stuffed inside the duct insulating the heater from the environment.

A thermocouple measures the heater outlet temperature of the hydrogen, and the Eurotherm controller adjusts the duty cycle of the heater depending on the temperature and set point. Additionally, a handheld thermocouple reader measures the outside wall temperature of the heater to ensure that the flammability limit of hydrogen is not reached.

#### 4.3.1.3 Oxidant System Components

The oxidant system contains a few slightly different parts due to the way air is supplied and the fact that it is not dead-ended as is the hydrogen. Similar to the fuel system, the part numbers in the following sections correspond to the system drawings located in Appendix 2 figures 4 and 6.

Compressor (A-1)

The air compressor was donated by Ingersoll-Rand. The OL5 compressor is an oil-free, single-stage, piston-cylinder compressor with an aftercooler. It can produce a maximum of 27 acfm, which is transferred into an approximately 60 gallon tank. It has a pressure switch set for approximately 125 psig. The compressor is mounted on springs to dampen floor vibrations, and in order to reduce the noise level, a sound barrier was built around the compressor.

The barrier consists of two 4 foot frames lined with sound absorbent and reflecting material. The inner barrier has an 18 inch space along the bottom to allow air to flow to and from the compressor. The outer barrier starts at the floor and rises 4 feet. The combination of the two barriers forces air and sound to travel to the floor and then up, and all of the surfaces are covered with sound dampening material. This barrier reduces the noise level measured near the display board from 100 dB to 80 dB, which is only 8 dB above the 72 dB base level, which is measured with the compressor off.

Air Heater (A-8)

Omega Engineering manufactures the AHPF-081 heater for the air from 316 stainless steel. The in-line heater is only capable of 267 SLPM (15 cfm @ approximately 100°C and atmospheric pressure), but the maximum flow rate of air is 500 SLPM. Therefore, a bypass around the heater allows large flow rates to be managed. The 600 Watt heater is powered by a 120 VAC circuit and is regulated with a heater controller. The heater is not recommended for flow rates less than 32 SLPM

Back-Pressure Regulator (A-28)

The pressure in the air line is regulated by a stainless steel Fairchild 66BP backpressure regulator. The regulator can handle flows up to 650 SLPM (23 scfm), which is greater than the required maximum flow rate of 450 SLPM. The regulator has ¼" FPT connections, and it has a knob for adjusting the pressure.

### 4.3.2 Coolant System Components

The assembly of the coolant system requires careful attention to the cleanliness

and reactivity of all parts. The coolant water must be kept at very high resistivity levels ($\geq$2 MΩ-cm). For this reason, only parts with corrosion resistance greater than or equal to that of 316 stainless steel are allowed in the system. The tubing connecting all components is ¾" 316 stainless steel with a wall thickness of 0.035".

#### 4.3.2.1 Coolant reservoir (C-1)

The reservoir was manufactured from 316 stainless steel to our specifications. As shown in Figure 4-5, it contains one ¾" threaded port at the bottom of the tank for an outlet, one 2" threaded port on the side of the tank for the immersion heater, three more ¾" ports on the side of the tank for a level switch, resistivity sensor, and the line return, and one ½" threaded side port for a temperature measurement. Additionally, on the top of the reservoir, a 1 ½" port provides a vent and filling location.

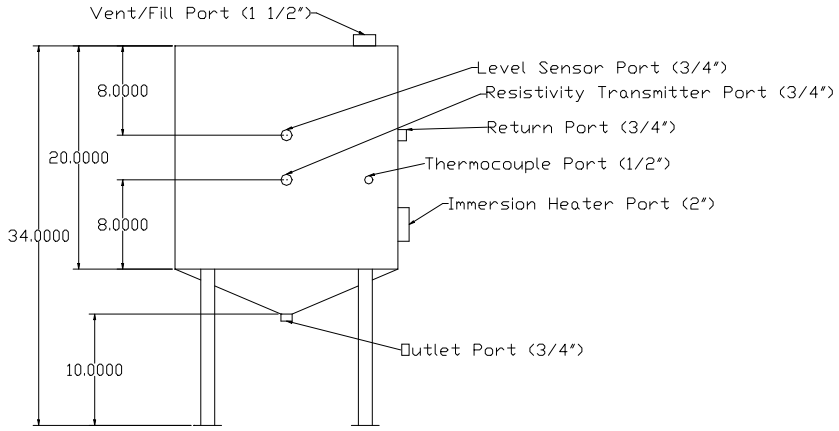


**Figure 4-5. Coolant reservoir schematic**

#### 4.3.2.2 Heater (C-1b)

The 3 kW Chromolox immersion heater in the reservoir has 316 stainless steel wetted parts. Figure 4-6 shows a wiring schematic for the immersion heater control system. It requires 480 Volt single-phase power, which is connected through a definite-purpose contactor that is powered by a Chromolox model 3101 high limit controller. The high limit controller monitors the temperature of the water and disengages the heater if

the temperature rises above the set point. The temperature is measured by a thermocouple inside a tube that projects into the water. The type T thermocouple is held in the tube with a highly heat conductive paste. Both the contactor and the high limit controller are powered by 24 VAC power.

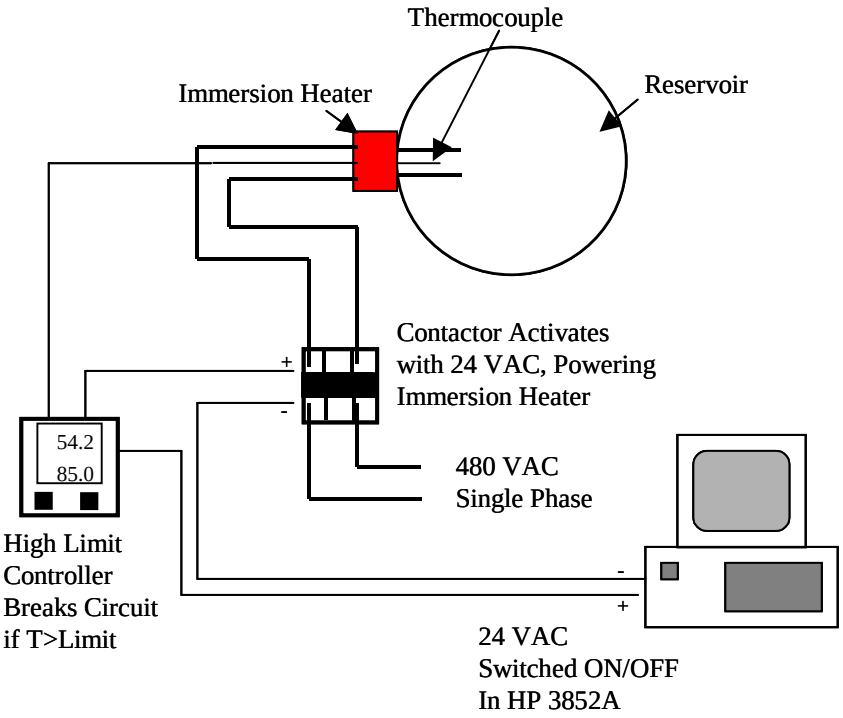


**Figure 4-6. Heater wiring schematic**

#### 4.3.2.3 Pump (C-3)

The pump, which is located just after the reservoir, supplies 24 liters per minute of coolant water to the apparatus. It is a ½ horsepower centrifugal pump powered by a 120 VAC circuit. All wetted parts are manufactured from 316 stainless steel.

#### 4.3.2.4 Flow Meters (C-11 and C-11a)

The original test apparatus design calls for a turbine flow meter, but the first implementation of the design required the substitution of a variable area flow meter. An Emco Turboline TLS flow meter was originally purchased to measure the flow of the coolant water. The Emco flow meter is capable of measuring flows from 0-5 gpm with an accuracy of ± 0.5 percent of the reading. The flow meter produces a 4-20 mA signal

that is read by the control program. This meter malfunctioned and was returned to the factory for inspection and repair.

A variable area flow meter was placed in the water line in order to provide a rough measure of flow. In addition, the stack pressure drop was correlated with the water flow rate. This correlation was used to determine the amount of water flowing through the stack during a test. The flow meter does not have adequate reactive properties to leave in the system while the stack is producing power, and, during a test, a length of 316 stainless steel tubing replaces the variable area flow meter.

#### 4.3.2.5 Resistivity Transmitter (C-6)

The RSTX-201-202 resistivity transmitter from Omega Engineering measures the resistivity of the water flowing out of the pump. The sensor, which was originally intended to be mounted in the reservoir, must be placed in such a fashion that the water flows directly over the electrode. The sensor measures the resistivity of the water from 0-20 MΩ-cm, and the transmitter converts that measurement into a 4-20 mA current signal. The sensor has a measurement sensitivity of 0.01 percent of the full scale (0.002 MΩ-cm) and a non-linearity of 0.125 percent (0.025 MΩ-cm).

#### 4.3.2.6 In-Line Deionizer (C-7)

To ensure that the water flowing through the fuel cell is sufficiently pure, a deionizing bed is placed in the coolant line. A Loeffler bagged filtration canister is used to hold a bed of deionizing resin through which the water is forced to flow. Teflon bags with 1 μm pores hold the resin in place. A short length of glass tubing directs the water through the resin preventing any water from flowing through the sides of the filter bag, as seen in Figure 4-7. The deionizing resin is suitable for use in high temperatures.

#### 4.3.2.7 Water Filter (C-8)

A double open-end filter canister prevents any contaminants from traveling through the line to the stack.. Filter cartridges rated for 20 μm are installed in the filter housing.

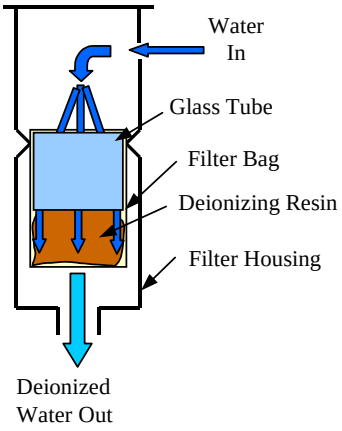


**Figure 4-7. Drawing of in-line deionizing bed**

#### 4.3.2.8 Heat Exchanger (C-9)

An Alfa Laval heat exchanger controls the coolant water temperature. The water-to-water counterflow heat exchanger can exchange 10 kW of power. Specifically, it is designed to cool 19 LPM of 60°C deionized water to 50°C. It consists of fourteen 316 stainless steel plates (each with an area of 25 $in^2$) brazed together with nickel. All four fluid connections are ¾" NPT.

#### 4.3.2.9 Level Sensor (C-1a)

The reservoir level is determined with the use of an Omega Engineering LVU-700 series ultrasonic level switch. This 316 stainless steel switch is installed through one of the ¾" NPT ports on the side of the reservoir. It closes a relay when water, due to its high density compared to air, sufficiently enhances the transmission of ultrasonic sound waves across a gap in the sensor. The closing of the relay causes a small voltage to be measured, which is interpreted as a full condition. The operation of the water heater is only enabled when the level switch indicates water in the tank. This reduces the risk of destroying the immersion heater.

#### 4.3.2.10 Differential Temperature Meter (C-12)

The differential temperature of the water across the fuel cell is an important measurement. It can be used to determine the amount of heat that the fuel cell is producing. An Omega DP26-TC differential temperature meter transmits the difference between two type T thermocouples to the data acquisition system as a 0-10 volt signal.

The meter is accurate to ±0.5°C.

#### 4.3.2.11 Control Valve (C-10)

A Johnson Controls VG-7000 ½" valve and VA-7152-1001 electric valve actuator adjusts the flow of cold water through the coolant heat exchanger. The actuator changes the position of the valve stem proportional to the applied 0-10 volts input signal.

### 4.3.3 Load System Components

A Dynaload RBL-100-600-4000 simulates an electric load placed on the fuel cell. It is capable of drawing up to 100 Volts, 600 Amps, and 4000 Watts of electrical power, which is dissipated by air-cooled resistors. The Dynaload is remotely programmable with a 0-10 volt signal representing zero to full scale of the user-selected options on the front panel.

The load can operate in one of four modes. First, the Dynaload can be set to draw a specified amount of current from the fuel cell. Similarly, it can pull power from the fuel cell at a preset voltage. It can also be adjusted to draw a specific amount of power from the stack. Finally, the load can act as a constant resistor across the fuel cell. The Dynaload will be used most often in the constant current and voltage modes. The constant voltage mode can be used to put a very small load on the stack for warm-up periods. After running the gas streams through the stack, the open circuit voltage can be measured, and in order to apply a small load, the load will be engaged at a voltage slightly below the open circuit. Polarization curves can be attained from fuel cells in the constant current mode by recording the voltage as the current is increased.

Table 4-2 shows the regulation and programming accuracy for the different control modes and voltage and current ranges. The accuracy is significantly better in the constant current and constant voltage modes. The current output signal, which is a 0-10 volt signal representing the selected current setting, has an accuracy of ±0.5 percent of full scale.

**Table 4-2. Electronic load regulation/programming accuracy**

| Control Mode | Voltage Range | | Current Range | |
|---|---|---|---|---|
| | 0-10 V | 0-50 V / 0-100 V | 0-20 A | 0-200 A / 0-600 A |
| Voltage | 0.15% / 0.5% | 0.15% / 0.25% | | |
| Current | | | 0.1% / 0.5% | 0.1% / 0.25% |
| Power | 3% of Full Scale / 3% of Full Scale | | | |
| Resistance | 3% of Full Scale / 3% of Full Scale | | | |

The Dynaload also has helpful protection limits that prevent it from being overloaded. It has a power limit of approximately 4250 Watts. The voltage and current are limited to 105 percent of the selected range for each, and the load is disconnected at voltages higher than the limit. Additionally, the load is automatically disconnected when the internal temperature exceeds 105°C. The device has two large fans that blow air from front to back cooling the electronics. Also, the cabinet in which it is mounted has a large fan, which removes the hot air.

### 4.3.4 Measurement/Control Components

The measurement and control of the fuel cell test apparatus are accomplished using a LabVIEW computer program. The computer has an Intel Pentium III 400 MHz processor with 64 MB of RAM. The LabVIEW programs controls an HP 3852A data acquisition mainframe and a National Instruments PCI-6713 analog output card. With these two instruments, all of the needed measurements and controls can be performed.

The control program serves four purposes. First, it records all the measurements made by the system during a test. Second, it is used to adjust the set point on certain devices. Next, it serves as a visual guide to the performance of the fuel cell during a test. Finally, the program makes key decisions that the operator is not able to make quickly enough. This task is given first priority in the program routine.

The cell voltages are the most important quantity that the program measures during a test. The life of the fuel cell depends on the program's ability to determine the condition of the individual cells in a stack. The cell voltages are measured directly from

the stack, but the overall stack voltage is measured across terminals on the electric load. The program looks at the cell voltages approximately every half second and determines if any cell has a voltage below 0.4 volts. This indicates a dangerous situation, and the load is disengaged.

#### 4.3.4.1 Control Devices

Hewlett Packard 3852A

The HP 3852A data acquisition mainframe has eight slots that can be filled with switching devices, relay multiplexers for voltage and thermocouple measurements, and analog output cards. The measurement and control system uses two HP 44708A thermocouple multiplexers and one HP 44725 switching card. The thermocouple cards can measure twenty thermocouples or signal voltages, and the switching card can independently switch on and off 16 channels.

The voltage and thermocouple measurements are made by connecting the leads of the two wires into a channel of the relay multiplexer. Current measurements are attached in the same manner, but a shunt resistor is soldered across the two points at which the mainframe makes its voltage measurement. In order to convert 4-20 mA signals to accurately measurable voltages, a 249Ω ±1 percent resistor shunts the voltage measurement resulting in a 0.996 V to 4.98 V signal corresponding to the 4-20 mA current.

The accuracy of the HP 3852A is very good for voltage and current measurements. The total system accuracy for voltage measurements in the 30V range is 0.008 percent of the reading plus 300μV. Therefore, a measurement of a 10 V signal would have an accuracy of ± 2.1mV or about 0.02 percent. The accuracy of thermocouple measurements is slightly different. The HP 44708A thermocouple multiplexer can read type T thermocouples with a total system accuracy of approximately 0.5 to 0.75°C within the range of 0 to 200°C.

The HP 3852A can read multiple channels very quickly. It should be able to read over 48 channels per second, but the interface between LabVIEW and the HP 3852A is

very slow. The LabVIEW and HP combination needed 0.4 seconds to make 1 measurement (only about 3 channels per second). The problem lies in the type of communication between the two systems, which is called GPIB. Currently, the program must formulate a message describing which channels to scan and send it to the HP 3852A. The HP receives the message and scans the channels quickly. Then, the LabVIEW program reads the data from the HP buffer. Finally, the program manipulates and interprets the data and starts the process again. LabVIEW is able to break down the time usage of each subroutine, and it indicated that the majority of time was spent reading the buffer on the HP 3852A. This suggests that the slow point in the process is transfer of data to LabVIEW.

Analog Output Card

A National Instruments PCI-6713 analog output card sends control signals to the various devices as controlled by the LabVIEW program. The card installs in the computer, and a 68 pin cable links the card to a connector block where all of the wires are attached. The NI PCI-6713 is capable of creating eight independent 0-10 Volt output signals with an accuracy of ± 0.0219 percent of the reading and an offset of ± 6 mV.

LabVIEW

LabVIEW is a visual based programming language designed for Windows. Lines of code are replaced with icons connected with "wires." Each icon has a different purpose and connections.

#### 4.3.4.2 Measurement Devices

Thermocouples

The test apparatus uses all type T (copper-constantan) thermocouples. The thermocouples are sheathed in a 1/8" 321 stainless steel tube, and the thermocouple bead is grounded to the sheath. Except for the coolant reservoir, all of the thermocouples are 3" long with a blue, two-pronged connector on the back end. The thermocouples are secured in the system with 1/8" compression fittings, which prevent any leaks. All thermocouple connections are made with 24 gauge type T thermocouple wire.

The thermocouples are read using the HP 3852A data acquisition system. The measurements are hardware compensated by a RTD directly on the multiplexer taking the reading. A command is given to the HP system to directly read the temperature indicated by the thermocouple. Therefore, the HP transfers the actual temperature, and no calculations must be made in the program.

Pressure Transducer

The four pressure transducers in the system are manufactured by Kobold. They all have ranges from 0 to 100 psig with a 4-20 mA signal. The transducers were purchased with an optional level of accuracy. These devices measure the pressure within ± 0.12 percent of the full-scale pressure. Therefore, the 100 psig transducers accurately read the pressure to within 0.12 psig. All wetted materials in the transducer are 316 stainless steel.

Relative Humidity Transmitter

The humidity level of the air and hydrogen are monitored with Vaisala HMP 230 relative humidity transmitters. The transmitters produce a 0-5 V signal proportional to the relative humidity (0-100 percent). These sensors have an accuracy of 1 percent RH at relative humidity levels below 90 percent and 2 percent RH at humidity levels above 90 percent. The sensor is 316 stainless steel with an end cap of sintered 316 stainless steel, which prevents the humidity-measuring device from being corrupted by any dust or water droplets. The transmitter is powered with 120 VAC.

### 4.3.5 Safety System Components

The safety systems are some of the most important in the entire test apparatus. Hydrogen is an extremely flammable gas, and proper precautions must be followed. To prevent hydrogen leaks from collecting at the ceiling, a vent hood covers the entire footprint of floor space in which hydrogen is present. The hydrogen in the fuel line is vented to the roof where a flame arrestor prevents any flame front from traveling down into the system. In the case of a serious hydrogen leak, alarms sensing the hydrogen concentration are placed just outside the vent hood and on the ceiling of the lab. At the sound of one of these alarms and at the operator's discretion, an emergency purge

releases the hydrogen and air present in the system to the atmosphere while replacing it with nitrogen. Activation of this purge also removes any load from the fuel cell.

#### 4.3.5.1 Hood

The hood was designed and constructed by the Virginia Tech Physical Plant. A 3150 cfm fan draws air from the test apparatus area and discharges it above the roof. The hood is 11' wide and 2' 9" deep.

#### 4.3.5.2 H2 Alarms

Two hazardous gas alarms detect hydrogen at 10 percent of the lower explosion limit, which is a mole fraction of hydrogen of 4 percent. The alarms are powered by 24 VAC and emit an audible alarm when the hydrogen concentration exceeds the limit.

#### 4.3.5.3 Nitrogen Purge

The nitrogen purge system is enabled by pressing a bright red button labeled "Emergency Stop." When depressed, a switch cuts power to the five solenoids in the gas streams and the 24 VAC transformer. A normally-closed solenoid at the entrance of each gas stream shuts in an emergency preventing the air or hydrogen from entering the system. Simultaneously, a normally-open solenoid at the exit of the fuel system opens, allowing the hydrogen previously blocked from escaping by a ball valve to exhaust to the atmosphere. Two more normally open solenoids start the flow of nitrogen through the two gas systems. The nitrogen enters each system just prior to the heating and humidification module. The nitrogen flow rate is controlled by a Dwyer Rate Master flow meter. The flow is metered to 0.27 SLPM per cell based on the published recommendations of the manufacturer for the fuel cell that was tested.

#### 4.3.5.4 Flashback Arrestor

A Superflash flash arrestor prevents any flame from traveling upstream to the test apparatus. The arrestor is placed at the exhaust of the hydrogen to the atmosphere. It can handle pressures up to 50 psig and flows well over 100 scfh.

# 5 TEST APPARATUS EVALUATION

The evaluation of the designed and constructed test apparatus encompassed many different procedures. First, the individual components were calibrated or tested to ensure proper operation. Next, the major systems were run individually making sure that all of the components worked as they were intended and that the program performed as intended. Finally, the test apparatus was applied to determine the polarization curve for a 5-cell 1 kW fuel cell stack manufactured by Energy Partners, Inc.

## *5.1 Component Evaluation*

The measurement devices were evaluated to ensure proper operation. In most cases, the devices were factory calibrated, and testing consisted of verifying the functionality of the device. The pressure transducers, thermocouples, resistivity transmitter, level sensor, and relative humidity transmitters were all tested to confirm proper performance. Additionally, the differential temperature meter was calibrated.

### 5.1.1 Pressure Transducers

The pressure transducers were checked at atmospheric pressure. First, all four of the transducers were positioned next to each other open to the atmosphere. The pressure was measured at each transducer, and they all agreed within 0.5 percent. Additionally, because the current measurements in the HP 3852A require soldering a resistor across the voltage measurement, the current readings on different channels could differ slightly. Therefore, one pressure transducer was measured on the eight different current sensing channels. The measurements differed by less than 1 percent. Additionally, all four of the pressure transducers were checked at higher pressures against pressure gauges.

### 5.1.2 Relative Humidity Transmitter

The two Vaisala relative humidity transmitters were more difficult to evaluate. A dew point hygrometer was used to check the precision of the Vaisala instruments. Humidity measurements at atmospheric pressure were compared and found to agree within 10 percent. The manufacturer performs calibration of these instruments, but the present calibration is more than three years old. Therefore, the relative humidity

measurements are not regarded as precise. The instruments were used to determine if the humidity was above approximately 85 percent and at a constant level.

### 5.1.3 Mass Flow Meters

While the manufacturer calibrated the mass flow meters, their functionality was checked by observing the pressure drop in the air compressor tank. The ideal gas law was used to estimate the volume of the tank by reading the pressure difference (220 kPa ) on the tank over a five minute period while the mass flow meter allowed a constant mass flow rate (100 SLPM) to leave the tank. Assuming a tank temperature of 22°, it was determined that the tank volume was approximately 60 gallons. The air compressor tank is approximately 60 gallons suggesting that the mass flow controllers were operating correctly.

### 5.1.4 Resistivity Transmitter

The resistivity transmitter for the coolant water was calibrated by the manufacturer, but it was checked for proper operation with a handheld resistivity meter. First, the handheld meter was calibrated using a standard fluid at 11.9 kΩ-cm. The flow of water was occasionally diverted from the line into the handheld meter. The resistivity transmitter and the handheld meter were confirmed to read similar values.

### 5.1.5 Differential Temperature Meter

The differential temperature meter was calibrated in an ice slurry using the meter's built-in calibration procedure. The two thermocouples were placed in the ice, and the value on the meter was adjusted to read 0°C for each thermocouple. The calibration was confirmed by placing the thermocouples together in the same environment and observing a differential temperature of 0°C.

### 5.1.6 Level Switch

Because the level in the tank was not visible, the level switch was confirmed to perform correctly by adding water into the tank until the switch reacted to the water being above its level. Water was then drained from the tank until the level switch confirmed that water dropped below the sensor, which took very little water. Finally, a small

amount of water was added again until the switch confirmed that the water level was above the sensor.

## 5.2 System Evaluation

The evaluation of the different systems incorporated several different phases. First, the systems were checked for leaks. The control routine for each system was also appraised. Finally, the entire system was run individually to confirm adequate performance.

### 5.2.1 Fuel

The fuel system required the removal of as many leaks as physically possible, due to the explosive nature of hydrogen. The leak test was performed by running air through the system with the exhaust valve fully closed. At first, the mass flow meter showed a significant flow of gas through the system. The system was then kept at a constant pressure (approximately 80 psig) while Snoop™ was applied to all compression fittings and threaded fittings. Generally, leaks were found in large threaded fittings (larger than 1") and some welded components. The threaded fittings were removed and wrapped with heavier Teflon thread seal tape. The leaky welded components were rewelded to our satisfaction. The spray chamber and drain traps were leak tested separately to ensure that any leaks encountered did not originate in those components. All major and minor leaks were removed, but some extremely small leaks were still present. These leaks were not detectable with Snoop™. The final pressure test showed a pressure loss of less than 0.1 psi per minute.

The fuel system performance was also checked with air flowing through the lines instead of hydrogen. The air was run at 50 SLPM (according to the hydrogen mass flow meter) and 101 kPa gauge. The heater outlet temperature was controlled to 100°C to ensure proper operation of the heating unit. After the line temperature near the fuel cell inlet was observed rising slowly, the heater outlet temperature setting was raised to 150°C. When the line temperature near the fuel cell inlet reached 90°C, the humidification water was added to the system. The differential pressure between the nozzle gas and line gas was set at approximately 30 psi, and the humidification water

flow rate was set at its lowest possible value (< 0.5 gph). The temperature was observed to drop as the humidity level increased, and after a long start up period, the temperature increased while the relative humidity stayed above 90 percent. The system kept a temperature of approximately 70°C and 90 percent RH for about 1 hour. These conditions were more than acceptable, and the fuel system was determined to be acceptable for stack testing.

### 5.2.2 Oxidant

The oxidant system was actually tested before the fuel system, and many of the same observations were made. However, the leak test for the oxidant line was not as intense. Most leaks in compression fittings and threaded fittings were removed. A pressure test revealed some leaks in the system, but very small leaks that were not obvious were left alone.

The heating and humidification components on the air system were extensively tested. The final design of the air and hydrogen systems were developed as trial and error experiments on the air system. After the original design failed to produce air at the acceptable temperature and humidity levels, a rope heater was added on the short length of tubing between the spray and separation chamber. This design change resulted in air at 60°C and +93 percent RH near the fuel cell inlet with a mass flow of 100 SLPM and pressure of 101 kPa gauge. This was achieved with the heater outlet temperature set at 200°C. With an acceptable heating and humidifying capacity and all measurements and controls working properly, the oxidant system was determined to be ready for performance testing of fuel cell stacks.

### 5.2.3 Coolant

The coolant system was also extensively tested prior to the test apparatus performance evaluation. First, the control of the immersion heater was tested with the power to the heater turned off at the breaker. The high limit controller was turned on, and the control program was given a set point of 50°C. The definite-purpose contactor was observed to switch on. The set point was then changed to 20°C (below the actual temperature), and the contactor disengaged. Next, the control set point was returned to

its 50°C setting, and the high limit controller was set with a high limit less than the tank temperature. Again, the contactor was observed to disengage. Finally, the heater power was applied, the high limit controller was set at 80°C, and the control program was set to control the tank to a temperature of 50°C. The heater slowly heated the water, and when the temperature reached 50°C, the program disengaged the heater as required.

The coolant temperature control system was then tested. With the tank temperature at approximately 50°C, the pump was started, and the hot water flowed through the coolant line. The control program was set to control the fuel cell outlet temperature to 45°C. Unfortunately, the test system did not approximate the fuel cell stack very well. During the evaluation, no heat was added to the water. As the control program would begin to cool the water, the tank temperature would drop and the temperature difference would become too small to adequately control the coolant temperature. At these low levels, the control valve would either be slightly on, cooling the water too much, or off, which did not cool the water at all. In an actual testing situation, the fuel cell stack would increase the temperature of the water a few degrees, and, as a result, the differential temperature between the tank and coolant water would require a greater city water flow through the heat exchanger making control easier. An attempt was made to limit the flow of the city water by installing a globe valve at the drain. While this helped significantly, controlling the outlet temperature was still difficult for the same reason.

Actually, the temperature could be controlled accurately by manually adjusting the control valve position, but when the program controlled the valve position, the outlet temperature could not be kept at a steady level. When the valve actuator failed twice, the decision was made to manually control the cold water flow by adjusting the globe valve position. This method, although it was not as simple as entering a value into the program, was reliable and effective. Finally, a flow curve for the pressure drop in the fuel cell stack was determined. This became necessary after the turbine in the turbine flow meter became jammed. The relationship between the flow rate and the pressure drop through the fuel cell can be used to determine the flow rate during a test.

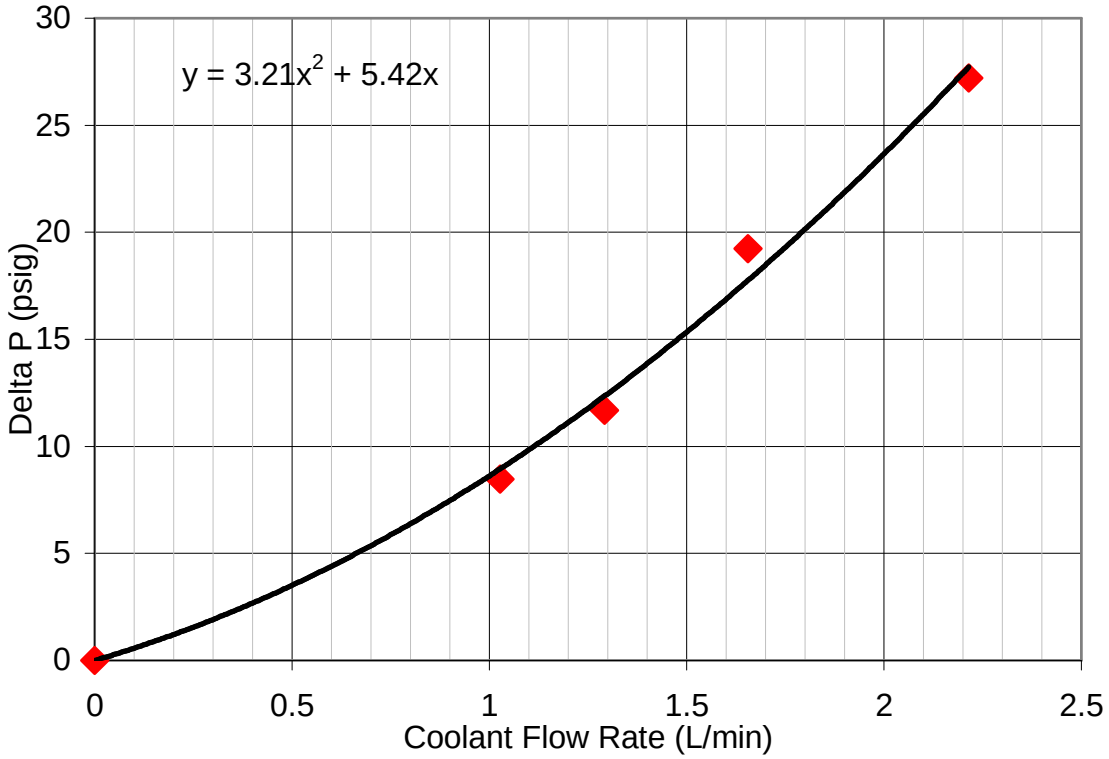


**Figure 5-1. Pressure drop vs. coolant flow rate for EP 5-cell stack**

The flow curve was determined by monitoring the pressure drop through the fuel cell. An approximate flow rate was set using the Dwyer flow meter, and, when the pressure drop became steady, the return line was redirected into a 4 liter graduated cylinder for a set period of time. The Figure 5-1 shows the flow curve for the Energy Partners 780 $cm^2$ 5-cell stack.

These evaluations confirmed that the coolant system could be used to reliably and effectively measure and control the necessary variables. The system was ready for stack testing.

### 5.2.4 Load

The load system was thoroughly tested to ensure that the correct load was applied to the fuel cell and that the load could be removed from the fuel cell in sufficient time in the event of an unhealthy stack condition or an emergency. First, the programmable load was manually tested to ensure proper working order. A 12V battery was connected to the load, and power was drawn from the battery both in the constant current setting and in the

constant voltage setting. Next, the load was controlled remotely with a LabVIEW program. Both the load and program functioned well under remote operation. Finally, the ability to remove the load was examined using the same battery and a 1.5 V battery to simulate the cell voltages. When the 1.5 V battery was disconnected, the programmable load quickly disengaged as required. When the emergency stop button was depressed, the load disengaged, but load was removed at a much slower rate. It took approximately 4 seconds to fully remove the load. This was an acceptable, but not preferred, condition. Therefore, the load system was determined to be ready to test a fuel cell stack.

### 5.2.5 Safety

The main safety system requiring evaluation is the purge system. The purge was first checked for leaks. Then, after passing the leak test, the emergency stop button was pressed while air ran through the oxidant system and nitrogen flowed through the fuel system. Additionally, the programmable load was connected to a battery and set to draw power from it. When the button was pressed, the flow of air and nitrogen as the fuel gas stopped and the nitrogen as the purge gas flowed through the entire system. It was noticed that the pressure on the air side was approximately 70 kPa higher due to the backpressure regulator, but this was an acceptable condition considering that more nitrogen would flow through the anode flow channels, which contain flammable hydrogen. All of the solenoids worked properly and quickly. The purge system was judged to be ready for stack testing.

## *5.3 Performance Evaluation*

The performance evaluation consisted of running all of the necessary systems simultaneously and using them together to draw power from a fuel cell stack. Due to the long start-up period for the gas heating and humidifying systems, they were started well in advance of the other systems. The heating of the water reservoir was begun several hours after the air and hydrogen were started. After achieving steady, acceptable conditions in the air, hydrogen, and coolant systems, the stack was connected to the test apparatus. The following procedure was used to start the testing process:

1. Leak test of the stack (completed previously)

2. Purge fuel system piping with nitrogen for 25 minutes at a flow rate of 43 SLPM

3. Close bypass (H-24) and purge stack at a nitrogen flow rate of 0.27 SLPM per cell (2.86 scfh total) for 5-7 minutes

4. Turn hydrogen and air heaters off and stop flow of humidification water to the humidifiers (gas conditions were 60°C and 95 percent RH)

5. Turn vent hood on

6. Close fuel exhaust ball valve (H-31) and pressurize stack to 5 psig with reactant gases.

7. Check hydrogen mass flow controller for a no-flow condition (small $H_2$ flow observed – 0.76 SLPM)

8. Measure open-circuit voltage (4.5 volts total)

9. Use $H_2$ detector to look for fuel leaks (none found)

10. Raise reactant pressures to 101 kPa gauge

11. Open fuel cell bypass 3-way valve (C-17) to allow coolant water into stack and set pressure drop to 138 kPa (corresponding flow of 1.6 lpm)

12. Visual check for water flow

13. Wait approximately 8 minutes for stack temperature to rise to acceptable level (46°C)

14. Open mass flow controllers to appropriate levels (10 SLPM for air and 1SLPM for hydrogen) for first current setting or higher

15. Apply load at constant current of 25A (watch performance for anomalies)

16. “Burp” fuel system every 30 seconds to 1 minute of power production to

refresh fuel supply throughout stack

17. Repeat steps 14-16 for different current settings (50, 100, 150, 160)

18. When finished testing, disconnect load bank slowly

19. Purge stack with nitrogen for 10 minutes at 2.86 scfh (0.27 SLPM per cell)

20. Allow stack voltage to drop below 10-20 percent of open circuit

21. Connect a 10 Watt power resistor to dissipate any excess voltage

22. Remove resistor at stack voltage less than 0.1 V

23. Finally, cap inlets and outlets to stack.

Using this procedure, a polarization curve was obtained for the Energy Partners 780 $cm^2$ 1 kW 5-cell stack. Figure 5-2 shows the data recorded during the test. Currents greater than 0.21 Amps per square centimeter caused the cell voltages to drop below the safety levels, and the load was disengaged. The figure shows all data points that were acquired. Because the data was acquired at a constant current, several points of slightly different voltages can be seen at each setting. A drop in stack voltage occurred when the system was operated dead-ended. As soon as the stack was "burped" (the valve at the fuel exhaust was opened for a short period of time), the stack voltage returned to its original value

The data was correlated an empirical equation proposed by Barbir et al. (3). The shape of the resulting polarization curve appears reasonable, but the maximum power drawn from the stack (432 Watts) was considerably less than the 900 Watts at which the stack was rated. The stack may operate better at higher operating temperatures and fuel pressures, but it is not likely that an increase of pressure or temperature would boost the power output by a factor of two. It is possible that the approximately 2 year period in which the stack was not operated could have affected the performance. There was a concern that the membranes may have dried during this period, which could have caused them to shrink, but the membranes were rehydrated prior to the test.

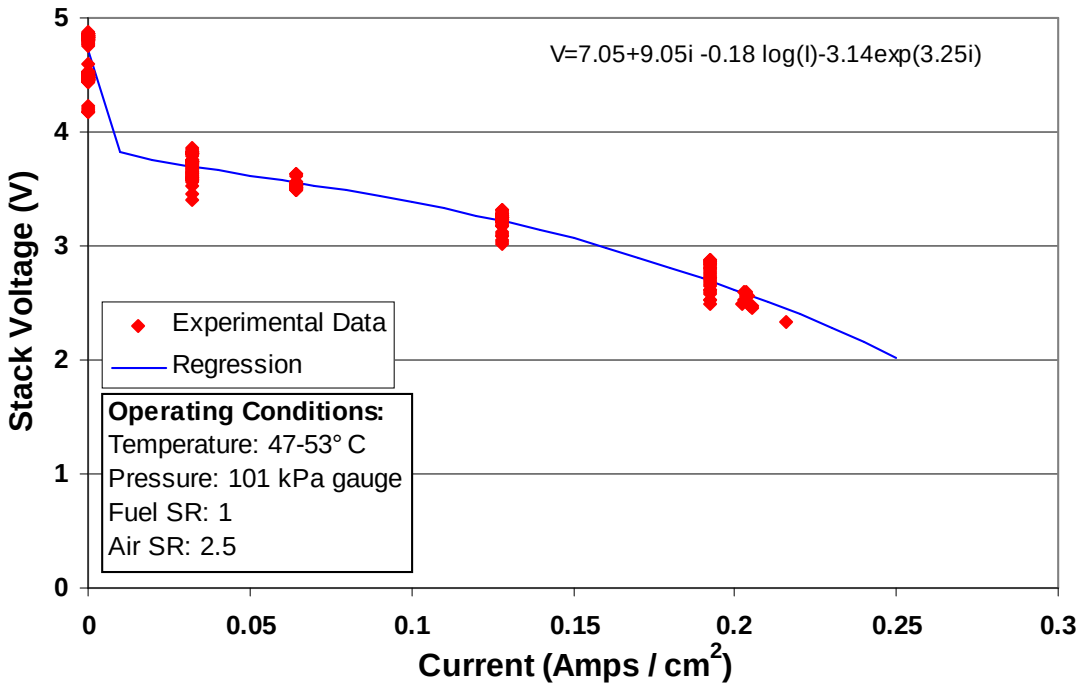


**Figure 5-2. Energy Partners 5-cell stack polarization curve**

The test apparatus proved effective at acquiring performance data from a fuel cell stack. However, during the test, the stack temperature varied from 47°C to 53°C. In fact, the coolant water was not cooled in any way in the heat exchanger. To simplify the operating procedure during the initial operation of the apparatus, the heating and humidification systems were not run during the actual test. However, the thermal capacitance of the system kept the gas streams at temperatures between 43°C and 37°C with relative humidities near 95 percent, and more importantly, the stack operating temperature stayed between 46 and 54°C. The safety systems adequately performed their duties. The cell voltage monitoring quickly disengaged the load when the stack was overloaded. Overall, the test apparatus performed its duties very well.

# 6 CONCLUSION/RECOMMENDATIONS

The design of the prototype test apparatus for proton exchange membrane fuel cells produced an effective and easy to use initial implementation. All four major systems performed their assigned duties well. The fuel and oxidant were supplied at an acceptable temperature and humidity level at relatively high mass flow rates. The coolant system produced clean, deionized water at the desired temperature and flow rate. A load was applied to a fuel cell at the appropriate time and value. Additionally, the load was disengaged whenever the cell voltages dropped below the preset limit. Most importantly, the test apparatus yielded a polarization curve for the test stack that had a form consistent with our expectations.

Although the test apparatus was able to acquire a polarization curve relatively easily, there are significant modifications and improvements that could strengthen its abilities. First, the heating and humidification systems for the gas streams need to be refined. The initial implementation and evaluation determined the maximum temperature and humidity levels that can be reached, but in order to make the apparatus more effective, the heating and humidification systems need to start-up quicker and provide improved controllability. The prototype heats the gases and relies on the flow of gas to bring the system up to temperature. At low mass flow rates, start-up times are long due to the thermal mass of the system. Furthermore, heat loss makes steady temperatures difficult to maintain. The hydrogen and air systems could be modified to heat the gas along the entire length of tubing. This would improve the temperature control and quicken the startup times. The humidity control could be improved by automatically adjusting the flow of water into the spray nozzles for each system. Automatic control would require rapid measurements of the humidity levels. Therefore, humidity sensors with a more rapid response and faster recovery from saturation need to be identified.

The coolant temperature must be kept at a constant value to accurately evaluate the stack performance. Presently, the circulating water temperature is too sensitive to changes in the control valve position. The water control scheme should be revised to operate the cooling water valve to maintain the heat exchanger discharge temperature.

The control scheme could be modified similar to that of the gas heater control. The LabVIEW program would simply send a set point signal to a independent controller. Also, a pressure-reducing valve should be installed on the city water line upstream of the control valve. Reducing the valve inlet pressure will slow the response of the system and may increase the life of the valve actuator.

Additionally, a deeper investigation into the slow communication between the measurement and control program and the HP 3852A should be performed. The combination of the two systems slowed the measurement speed considerably. The program may need to be streamlined, or the HP may need to be accessed in a different manner (possibly with VXI). The final option would be replacement of the HP system with a more LabVIEW compatible data acquisition system.

The measurement and control program could also be expanded to perform some additional functions. The display and logging of the individual cell voltages would provide the operator with a better understanding of the stack performance.

To improve the flexibility of the apparatus, a hydrogen recirculating system could be installed. The prototype is designed to run in dead-ended mode, but many fuel cell systems (especially transportation based) recirculate hydrogen. This feature would also minimize venting of hydrogen during start-up procedures. Implementation of a recirculating system would require a backpressure regulator and a recirculation pump. The addition of a recirculating system would allow the apparatus to run with fuel stoichiometries greater than one, which could improve stack performance.

Development of a fuel cell test apparatus that provides accurate data with a simple, flexible system for data acquisition and control is a formidable challenge. The prototype test apparatus developed here provides a useful means for measuring fuel cell stack performance. More importantly, it provides a foundation for on-going development of a fuel cell test facility. The experience and knowledge gained through the implementation of this apparatus will directly contribute to the development of a more advanced fuel cell test facility.

## REFERENCES


[1] Amphlett, J.C., et al., "Performance Modeling of the Ballard Mark IV Solid Polymer Electrolyte Fuel Cell, I. Mechanistic Model Development," *Journal of the Electrochemical Society*, Vol. 142, 1995, No. 1.

[2] Amphlett, J.C., et al., "Performance Modeling of the Ballard Mark IV Solid Polymer Electrolyte Fuel Cell, II. Empirical Model Development," *Journal of the Electrochemical Society*, Vol. 142, 1995, No. 1.

[3] Barbir, F., Balasubramanian, B., Neutzler, J., "Trade-Off Design Analysis of Operating Pressure and Temperature in PEM Fuel Cell Systems," *Proceedings of the ASME Advanced Energy Systems Division*, AES-Vol. 39, 1999, pp. 305-315.

[4] Bernardi, Dawn M. and Verbrugge, Mark W., "A Mathematical Model of the Solid-Polymer-Electrolyte Fuel Cell," *Journal of the Electrochemical Society*, Vol. 139, No. 9, 1992, pp. 2477-2490.

[5] Broka, K. and Ekdunge, P., "Modeling the PEM fuel cell cathode," *Journal of Applied Electrochemistry*, Vol 27, 1997, pp. 281-289.

[6] ElectroChem, Inc., FCT-2000 Test Station Modules web site, http://www.fuelcell.com/fct2000.html [visited 6-15-00]

[7] Hydrogenics Corporation, Products web site, http://www.hydrogenics.com/product-1.htm [visited 6-15-00]

[8] Lee, J.H. and Lalk, T.R., "Modeling Fuel Cell Stack Systems," *Journal of Power Sources*, Vol. 73, 1998, pp. 229-241.

[9] Marr, C. and Li, X., "Performance Modeling of a Proton Exchange Membrane Fuel Cell," *ASME Proceedings on Energy Sources Technology*, 1998.

[10] Nguyen, Trung V. and White, Ralph E., "A Water and Heat Management Model for Proton-Exchange-Membrane Fuel Cells," *Journal of the Electrochemical*

*Society*, Vol. 140, No. 8, 1993, pp. 2178-2186.

[11] Oetjen, H. F., et al., "Performance Data of a Proton Exchange Membrane Fuel Cell Using $H_2$/CO as Fuel Gas," *Journal of the Electrochemistry Society*, Vol. 143, No. 12, 1996, pp. 3838-3842.

[12] Springer, T. E., Zawodzinski, T. A., and Gottesfeld, S., "Polymer Electrolyte Fuel Cell Model," *Journal of the Electrochemistry Society*, Vol. 138, No. 8, 1991, pp. 2334-2342.

[13] Thirumalai, Dhanwa and White, Ralph E., "Mathematical Modeling of Proton-Exchange-Membrane Fuel-Cell Stacks," J. Electrochem. Soc., Vol. 144, No. 5, 1997, pp. 1717-1723.

[12] Yi, Jung S. and Nguyen, Trung V., "Proton Exchange Membrane Fuel Cells," *Journal of the Electrochemistry Society*, Vol. 145, No. 4, 1998, pp. 1149-1158.

# APPENDIX 1 – SYSTEM DRAWINGS

**List of Drawings** **Page**


1. Plan View of Ware Lab Bay 78

2. Front View of Display Board – All Systems Only 79

3. Front View of Display Board – Hydrogen System Only 80

4. Front View of Display Board – Air System Only 81

5. Front View of Display Board – Water System Only 82

6. Top View of Heating and Humidification Module 83

7. Coolant Water Module 84

8. Coolant Water Reservoir 85

9. Drain Trap 86

10. Spray Chamber Assembly 87

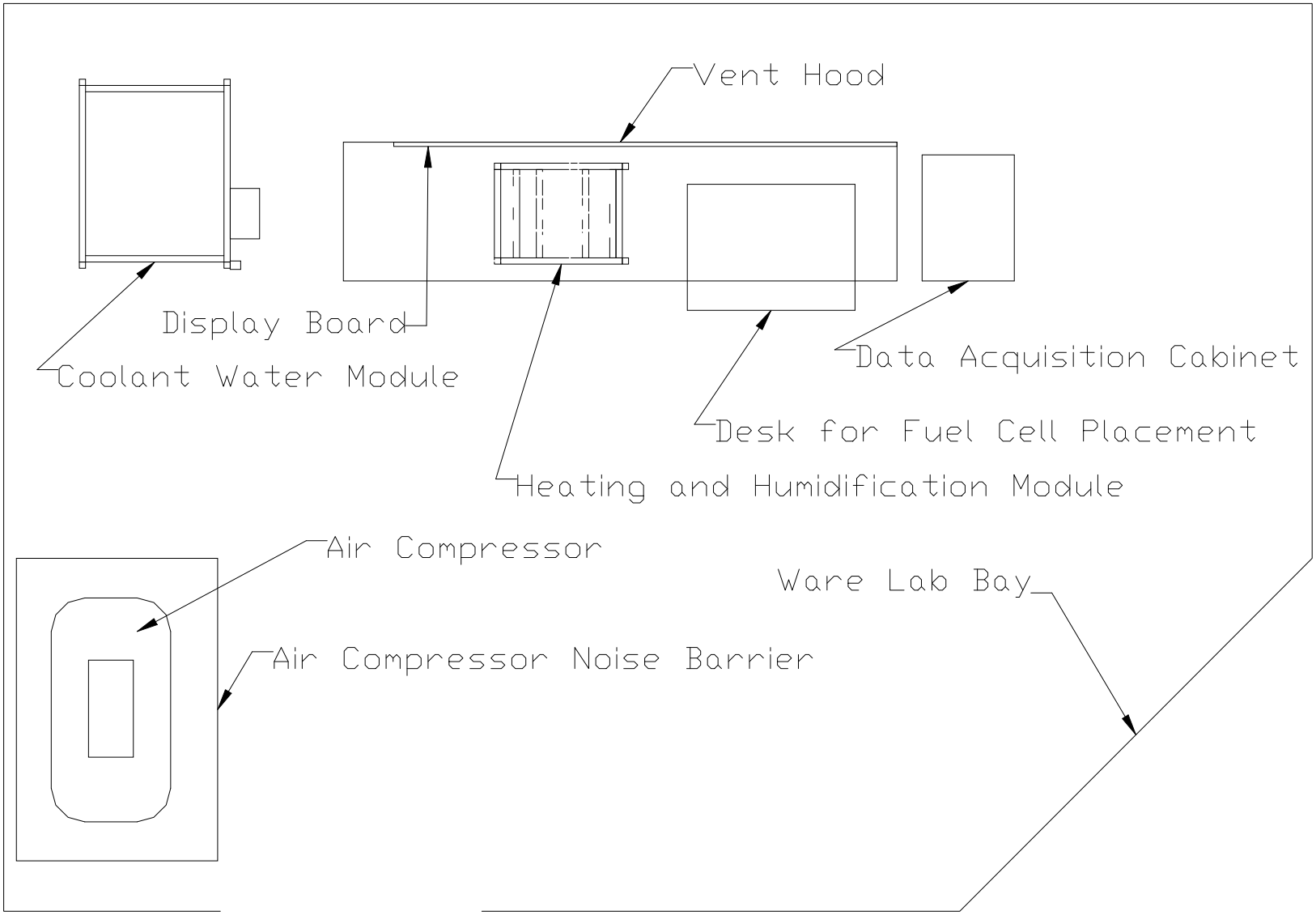


Figure 1. Plan view of fuel cell test apparatus in Ware Lab

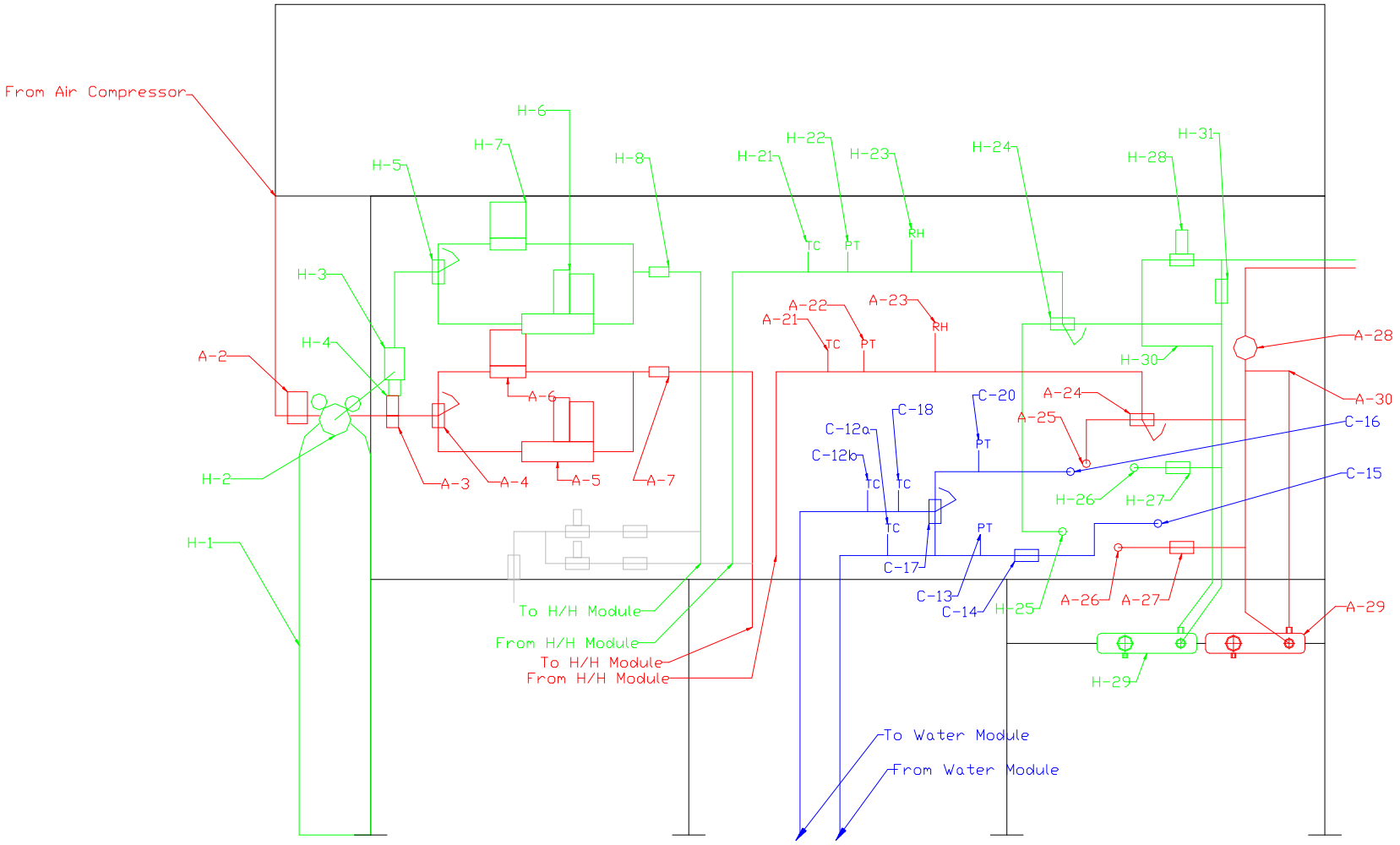


Figure 2. Front view of display board

| Hydrogen | Air | Coolant Water | Nitrogen |
|---|---|---|---|

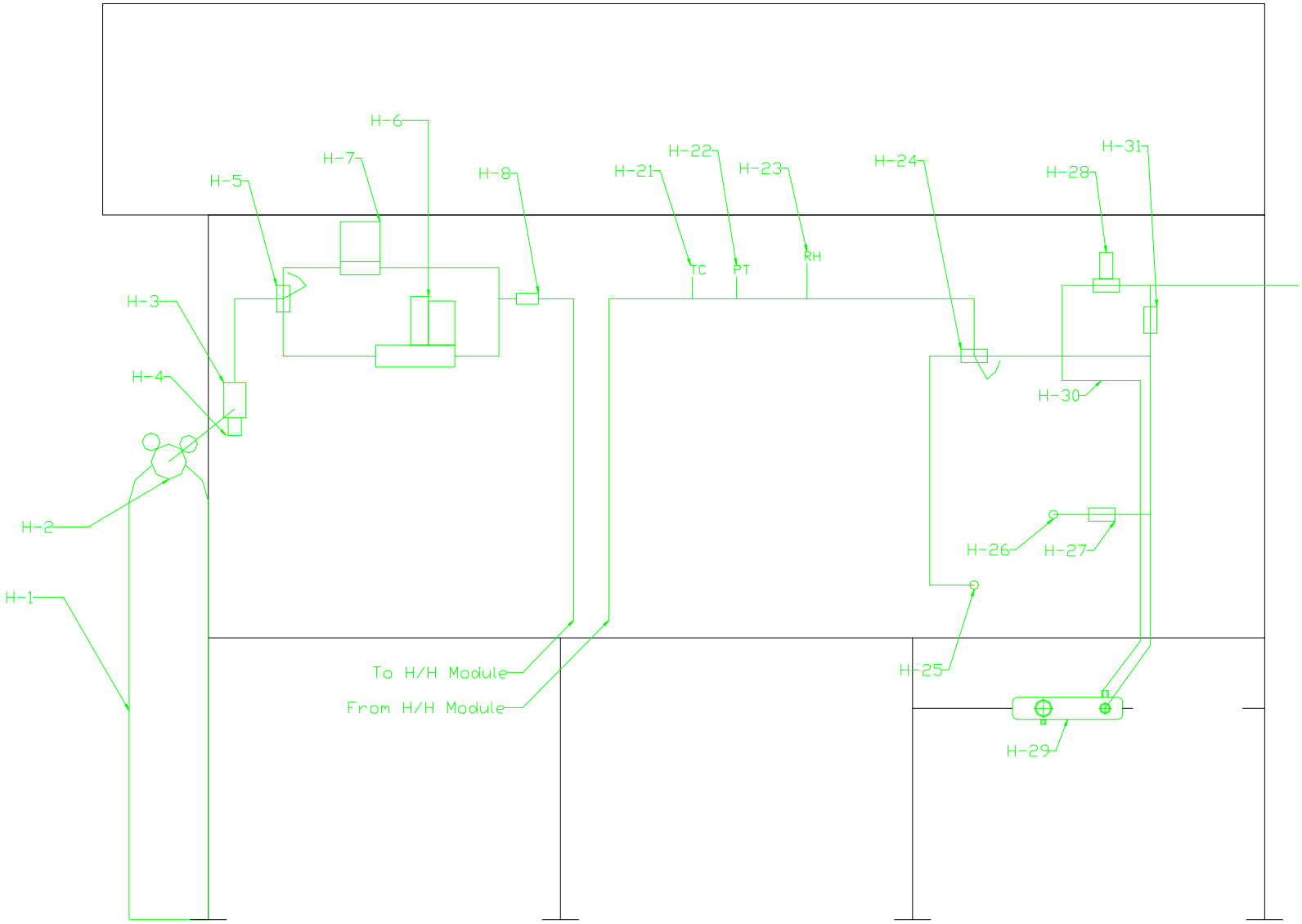


Figure 3. Front view of display board – hydrogen system only

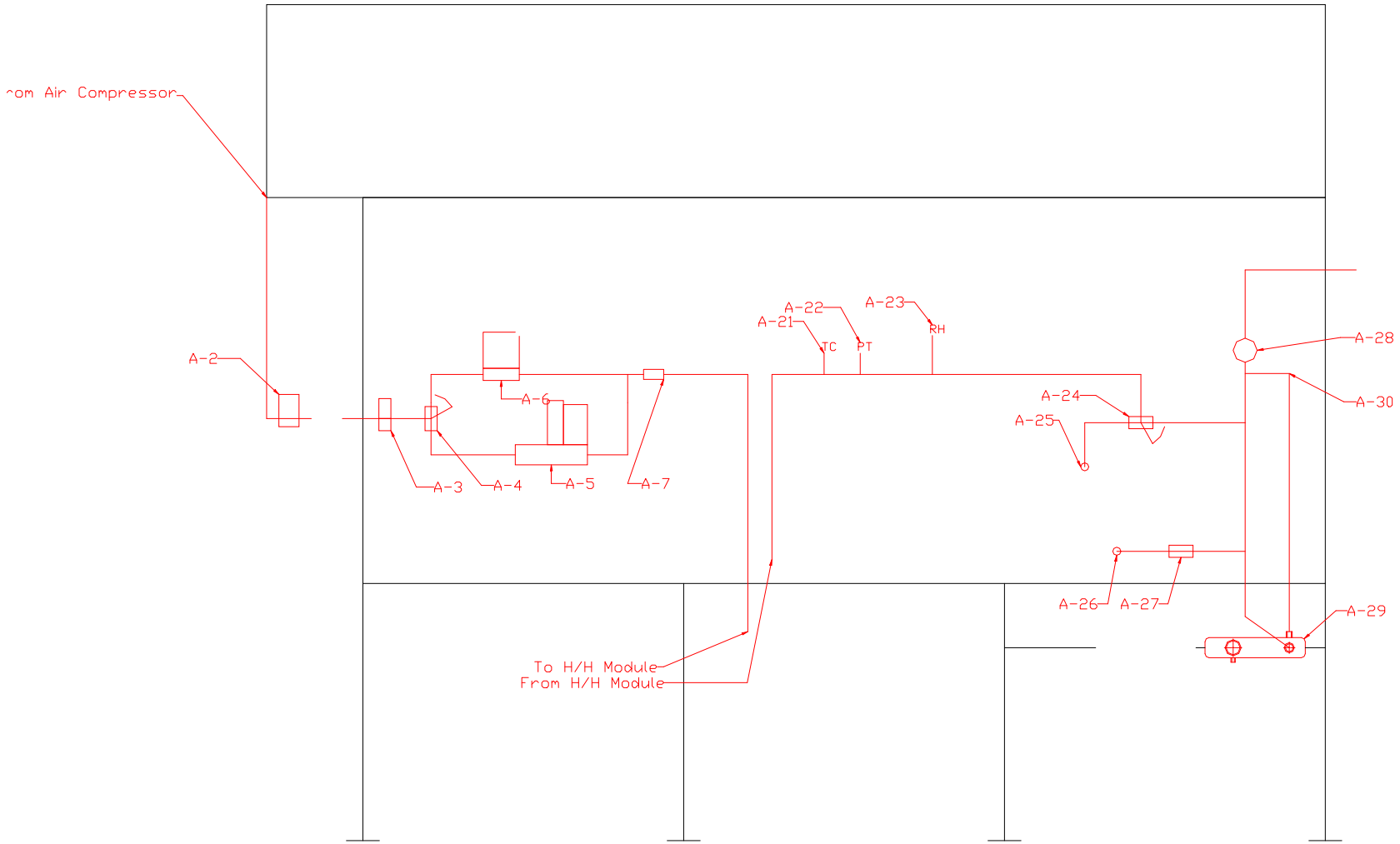


Figure 4. Front view of display board – air system only

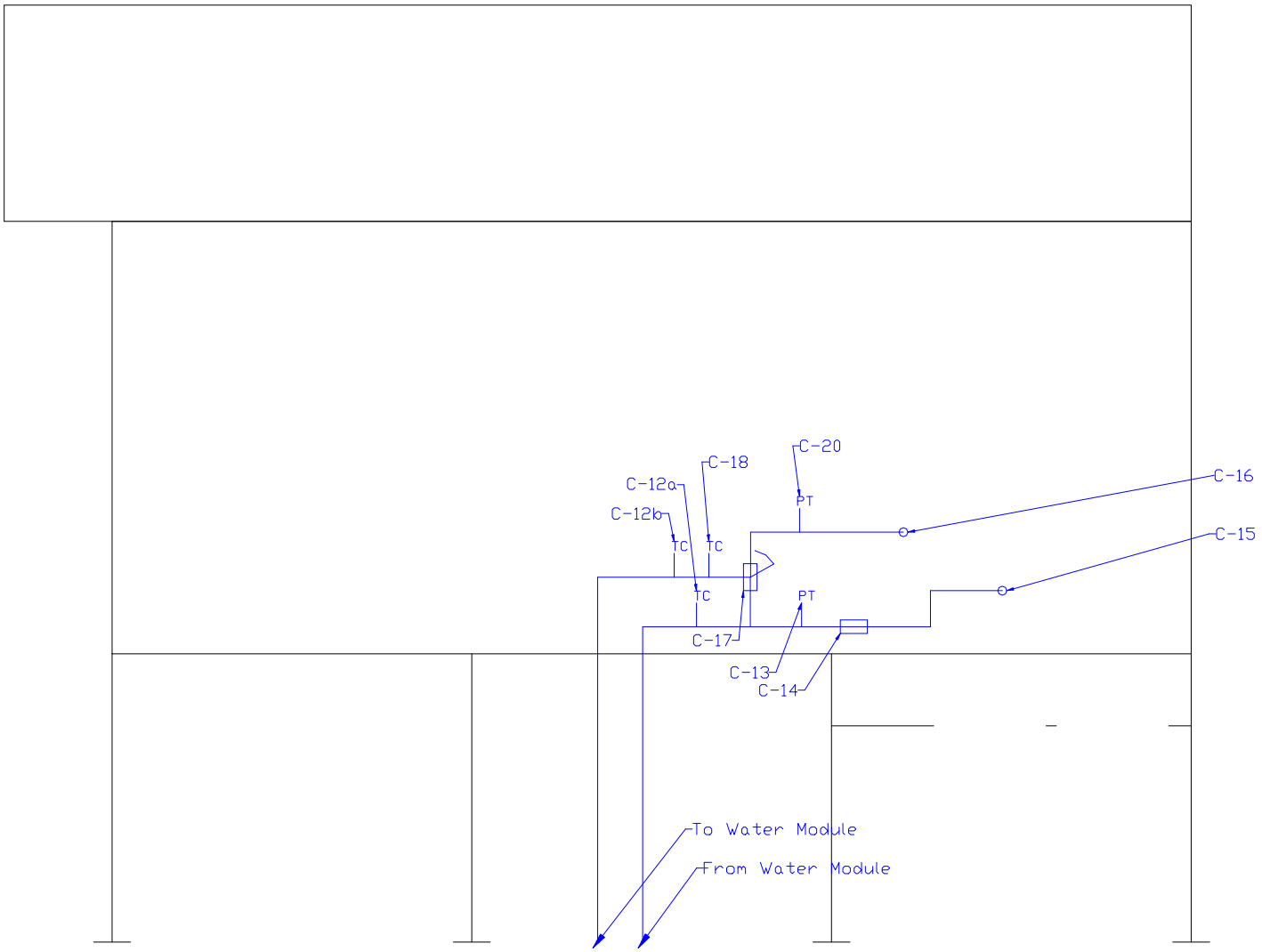


Figure 5. Front view of display board – coolant system only

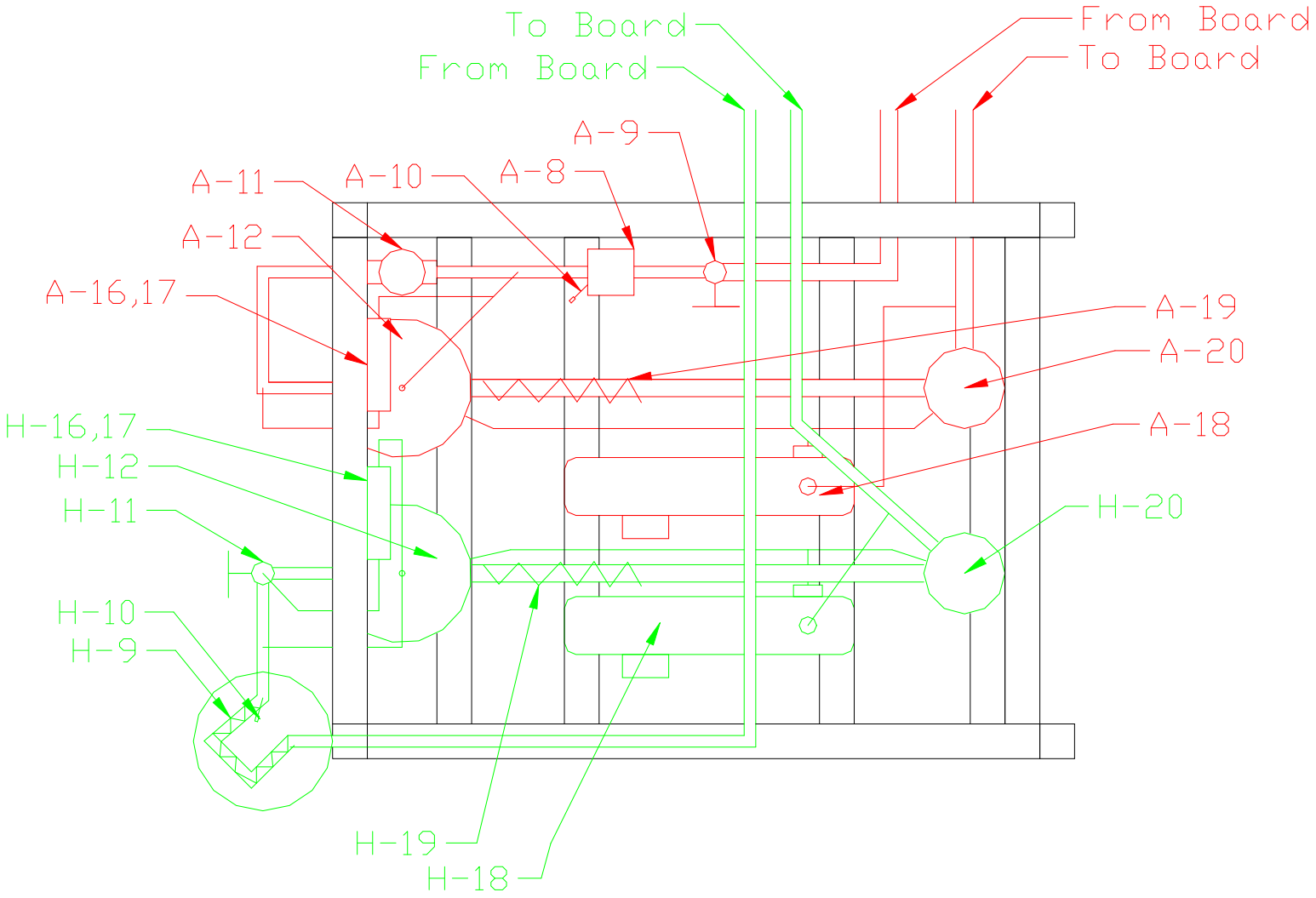


Figure 6. Top view of heating and humidification module

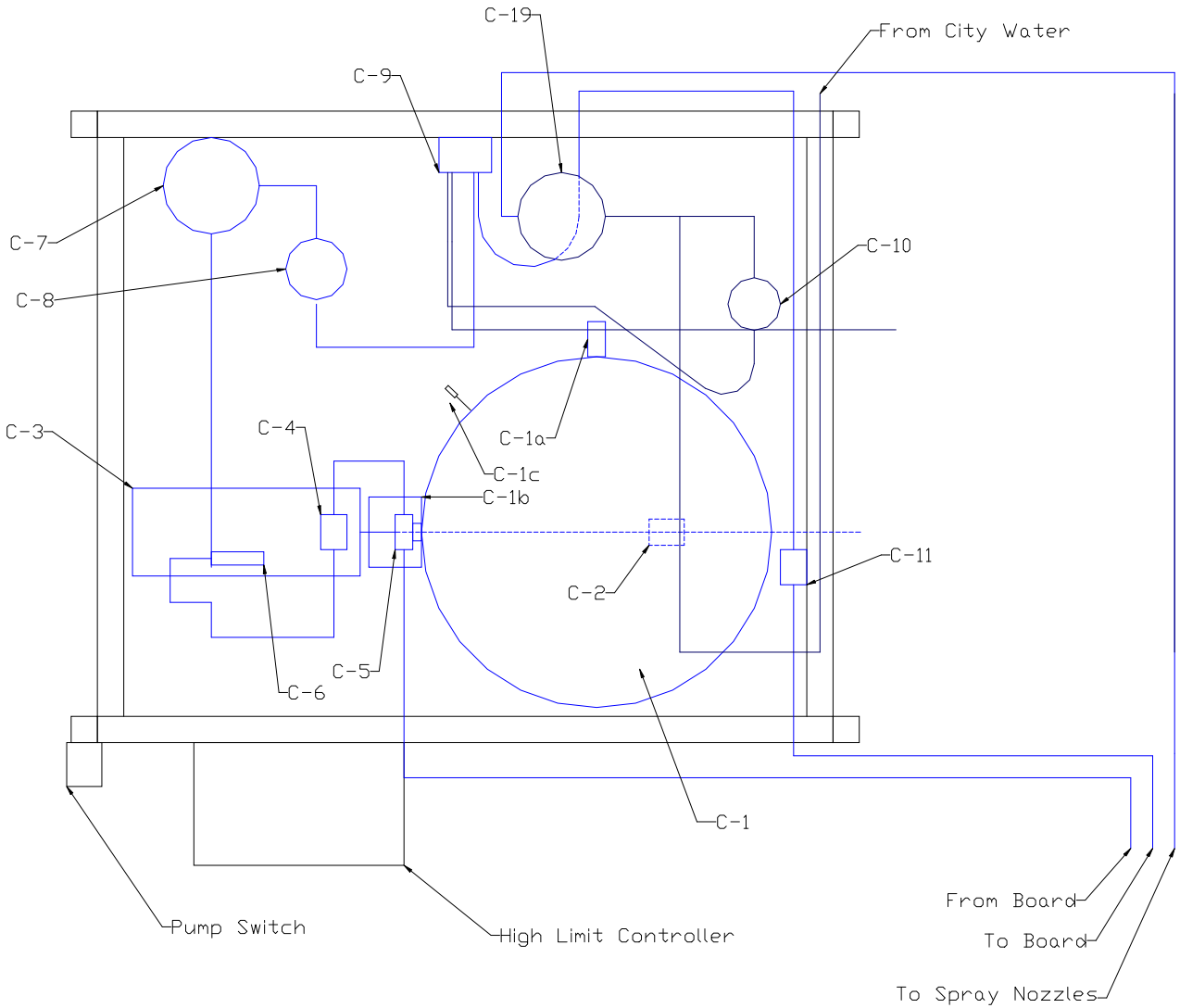


Figure 7. Top view of coolant water module

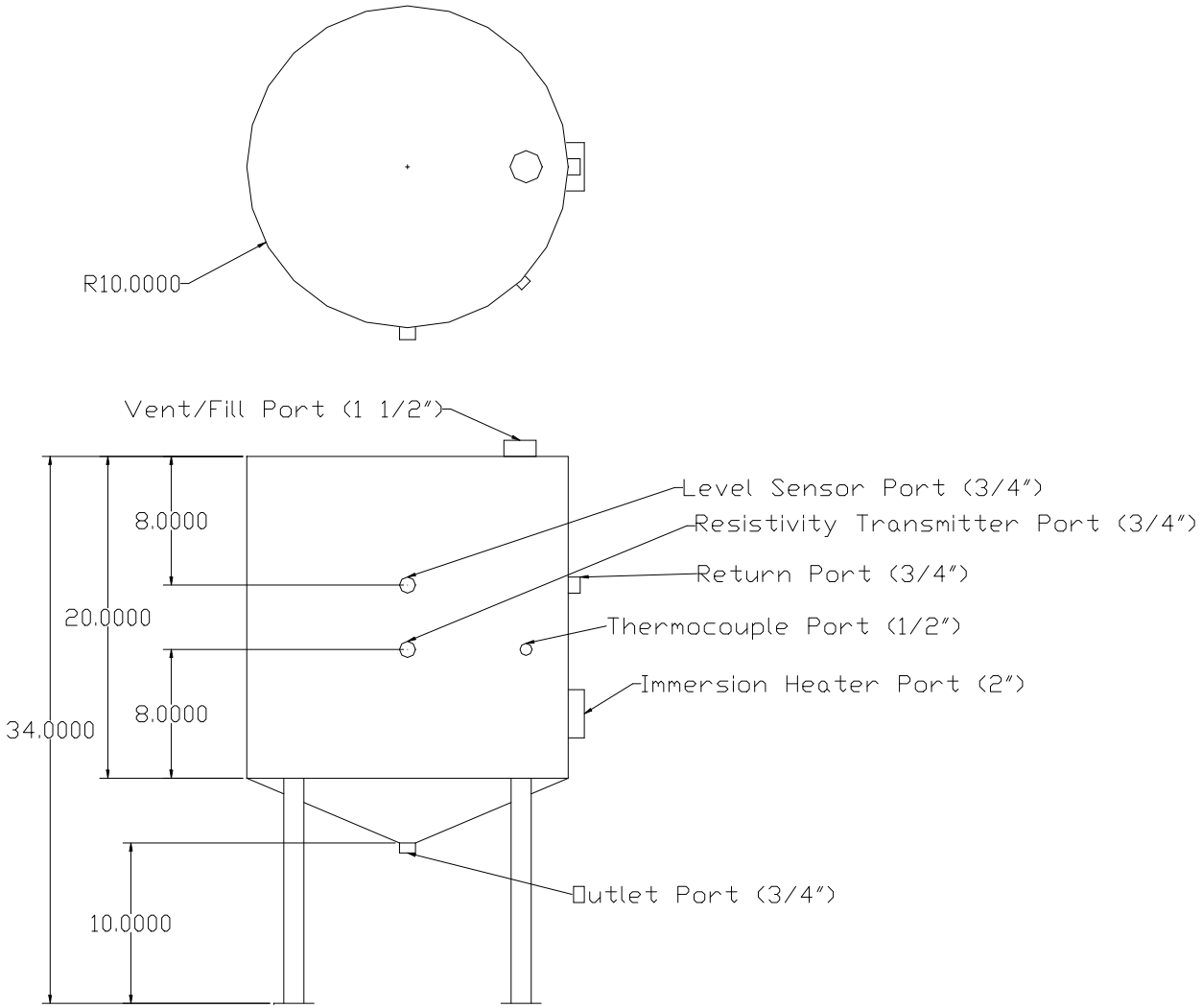


Figure 8. Coolant water reservoir

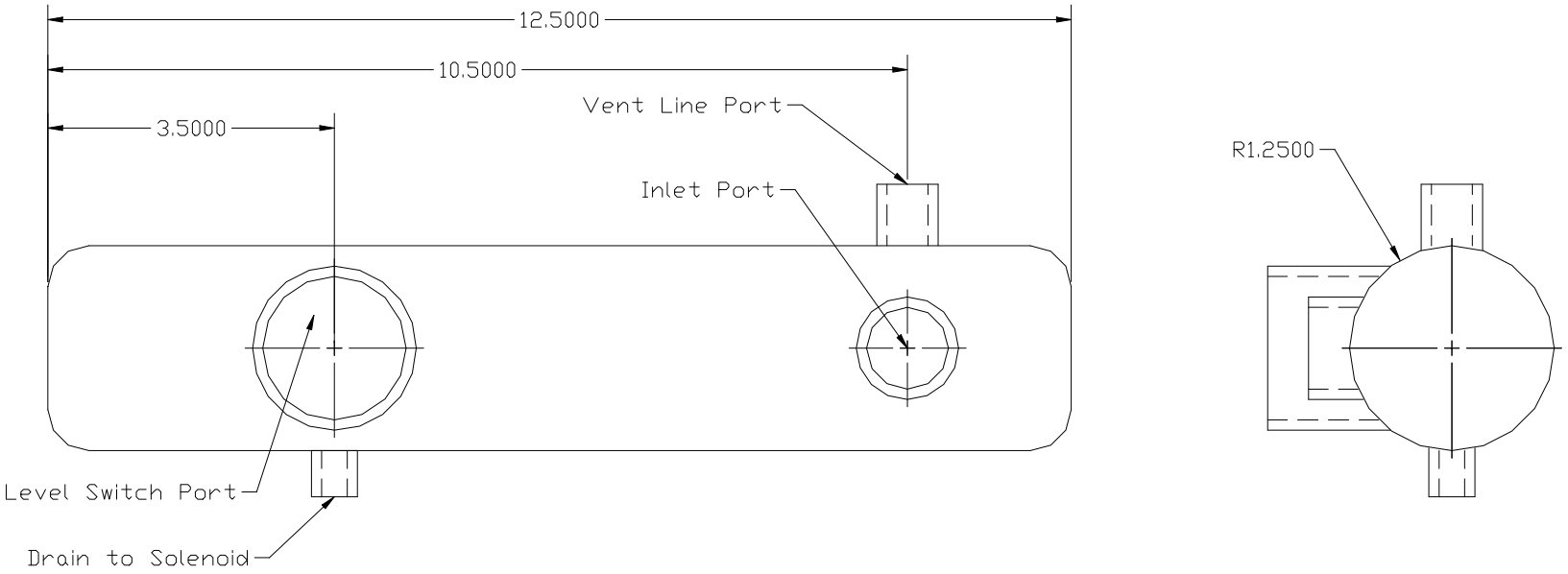


Figure 9. Drain Trap

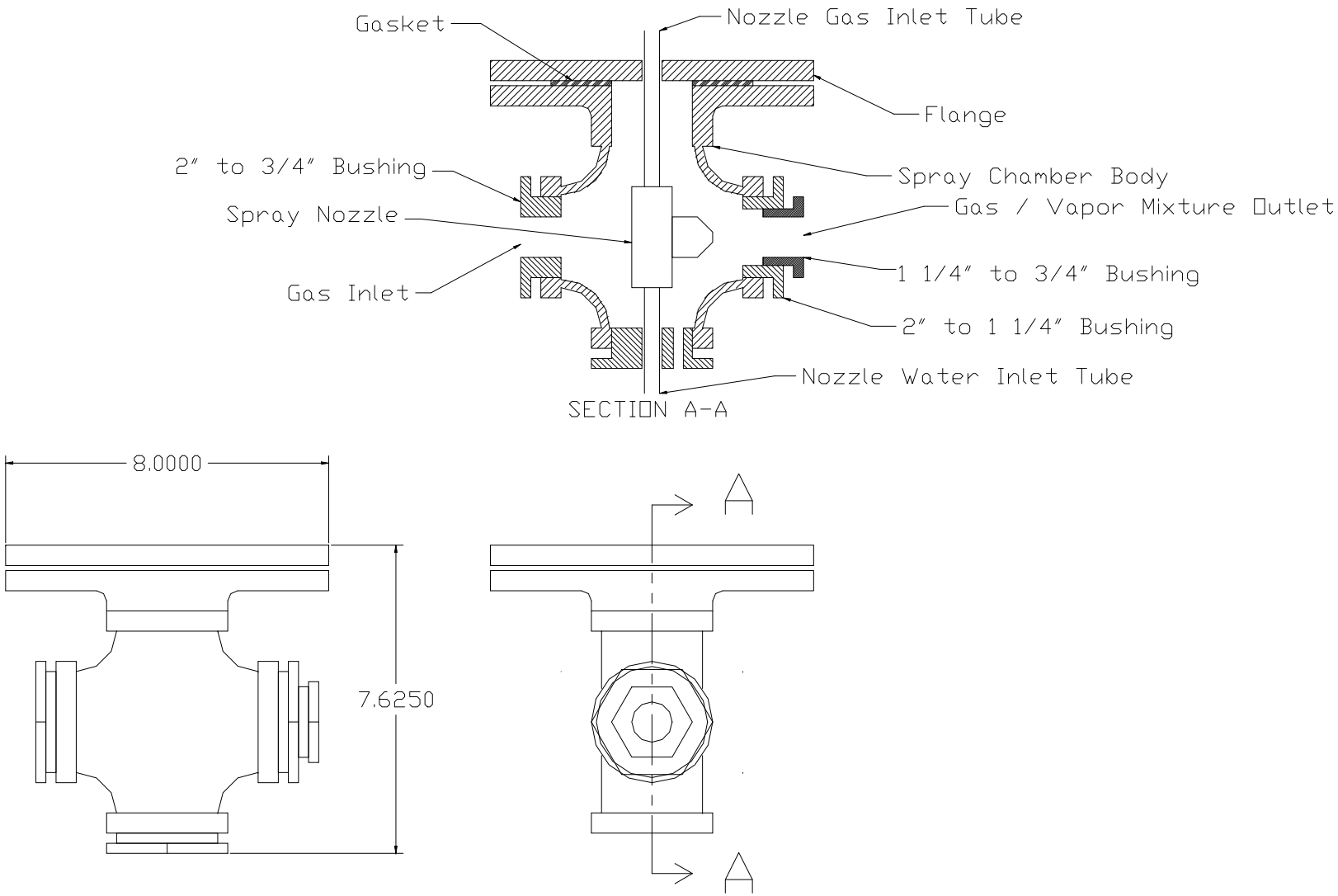


Figure 10. Spray Chamber Assembly

# APPENDIX 2 – PARTS LIST

## *Fuel System*

| System Part # | Description | Manufacturer | Model # |
|---|---|---|---|
| H-1 | Hydrogen Tank | Air Products | 1049 |
| H-2 | Regulator, brass | Concoa | CGA# 350 |
| H-3 | Solenoid – Normally Closed | | |
| H-4 | Filter Regulator | Watts | |
| H-5 | 3-way valve, ½", 316 SS | | |
| H-6 | High mass flow controller | Sierra | 840-High |
| H-7 | Low mass flow controller | Sierra | 840-Low |
| H-8 | Check Valve, ½", 316SS | | |
| H-9 | Rope Heater | Omega | FGR-060 |
| H-10 | Thermocouple | Omega | TMQ-321SS-G-3 |
| H-11 | Globe Valve, ½", 316SS | | |
| H-12 | Spray Chamber | | |
| H-12a | 2" 316 SS cross | | |
| H-12b | 2" 316 SS Flange | | |
| H-12c | Spray Nozzle | Bete | |
| H-13 | Ball Valve, ¼", 316SS | | |
| H-14 | Check Valve, ¼", 316SS | | |
| H-15 | Flow Meter w/ Valve | Dwyer | VVA-4 |
| H-16 | 3-way valve, 316SS, ½" | | |
| H-17 | Pressure Gauge | | |
| H-18 | Drain Trap | N/A | N/A |
| H-19 | Rope Heater | Omega | FGR-060 |
| H-20 | Separator | | |
| H-21 | Thermocouple | Omega | TMQ-321SS-G-3 |
| H-22 | Pressure Transducer | Kobold | KPG |
| H-23 | Relative Humidity Transmtr | Vaisala | HMP-233 |
| H-24 | 3-way Valve, ½", 316SS | | |
| H-25 | Fuel Cell Inlet | | |
| H-26 | Fuel Cell Outlet | | |
| H-27 | Check Valve, ½", 316SS | | |
| H-28 | Solenoid Valve, N.O., 316SS | | |
| H-29 | Drain Trap | | |
| H-30 | Vent Line | | |
| H-31 | Ball Valve, ½", 316SS | | |
| H-32 | Ball Valve, ½", Brass | | |
| H-33 | Flame Arrestor | SuperFlash | |

## *Oxidant System*

| System Part # | Description | Manufacturer | Model # |
|---|---|---|---|
| A-1 | Air Compressor | Ingersoll-Rand | OL5 |
| A-2 | Solenoid, N.C. ¾", 316SS | | |
| A-3 | Filter Regulator | Watts | |
| A-4 | 3-way Valve, ¾", 316SS | | |
| A-5 | High mass flow controller | Sierra | 840-High |
| A-6 | Low mass flow controller | Sierra | 840-Low |
| A-7 | Check Valve, ¾", 316SS | | |
| A-8 | Air Heater | Omega | APH-081 |
| A-9 | Globe Valve, ½", 316SS | | |
| A-10 | Thermocouple | Omega | TMQ-321SS-G-3 |
| A-11 | Globe Valve, ½", 316SS | | |
| A-12 | Spray Chamber | | |
| A-12a | 2" 316 SS cross | | |
| A-12b | 2" 316 SS Flange | | |
| A-12c | Spray Nozzle | Bete | |
| A-13 | Ball Valve, ¼", 316SS | | |
| A-14 | Check Valve, ¼", 316SS | | |
| A-15 | Flow Meter w/ Valve | Dwyer | VVA-4 |
| A-16 | 3-way valve, 316SS, ½" | | |
| A-17 | Pressure Gauge | | |
| A-18 | Drain Trap | | |
| A-19 | Rope Heater | Omega | FGR-060 |
| A-20 | Separator | | |
| A-21 | Thermocouple | Omega | TMQ-321SS-G-3 |
| A-22 | Pressure Transducer | Kobold | KPG |
| A-23 | Relative Humidity Transmtr | Vaisala | HMP-233 |
| A-24 | 3-way Valve, ¾", 316SS | | |
| A-25 | Fuel Cell Inlet | | |
| A-26 | Fuel Cell Outlet | | |
| A-27 | Check Valve, ¾", 316SS | | |
| A-28 | Back-Pressure Regulator | Fairchild | 66BP |
| A-29 | Drain Trap | | |
| A-30 | Vent | | |
| A-31 | Ball Valve, ¾", Brass | | |

## *Coolant System*

| | | | |
|---|---|---|---|
| C-1 | Reservoir | | |
| C-1a | Level Switch | Omega | LVU-700 |
| C-1b | Immersion Heater | Chromolox | |
| C-1c | Thermocouple | Omega | TMQ321SS-U-6 |
| C-2 | Ball Valve, ¾", 316SS | | |
| C-3 | Pump | MTH Pumps | T41C-SS |
| C-4 | 3-way Valve, ¾", 316SS | | |
| C-5 | Reservoir Return | | |
| C-6 | Resistivity Transmitter | Omega | RSTX-201-202 |
| C-7 | Deionizing Bed | Loeffler | |
| C-8 | Filter Housing | | |
| C-9 | Heat Exchanger | Alfa Laval | NB14-14H E21, E21 |
| C-10 | Electric Act. Control Valve | Johnson Controls | VG7000-VA7152 |
| C-11 | Turbine Flow Meter | Emco | Turboline TLS |
| C-11a | Variable Area Flow Meter | Dwyer | VVA-6 |
| C-12 | Diff. Temperature Meter | Omega | DP26-TC |
| C-12a | Inlet Thermocouple | Omega | TMQ321SS-G-3 |
| C-12b | Outlet Thermocouple | Omega | TMQ321SS-G-3 |
| C-13 | Inlet Pressure Transducer | Kobold | KPG |
| C-14 | Ball Valve, ¾", 316SS | | |
| C-15 | Fuel Cell Inlet | | |
| C-16 | Fuel Cell Outlet | | |
| C-17 | 3-way Valve, ¾", 316SS | | |
| C-18 | Outlet Thermocouple | Omega | TMQ321SS-G-3 |
| C-19 | City Water Deionizing Bed | Cole-Parmer | |

# APPENDIX 3 – OPERATING PROCEDURE

**Start-up**

1. Turn on main power at switch behind display board near data acquisition cabinet
2. Pull the emergency switch out to activate the purge solenoids
3. Start the LabVIEW program (pemfc.vi) – ensure that all controls are set to zero
4. Power the Eurotherm controllers and ensure that the air and hydrogen set points are below room temperature
5. Power on the Dynaload
6. Turn on the city water supply at ball valve above the water module
7. Open nitrogen bottle valve and regulate pressure to about 20 psig

Air

1. Set the air mass flow to 0 SLPM using the LabVIEW program
2. Switch on air compressor (A-1)
3. Turn 3-way valve (A-24) to bypass air around fuel cell
4. Change mass flow setting in LabVIEW to desired level
5. Adjust back-pressure regulator (A-28) to achieve desired pressure at transducer (A-22)
6. Adjust globe valve (A-11) on heating-humidifiying module to achieve a differential pressure (A-17) between the line and spray nozzle of approximately 30 psi

7. Change Eurotherm setting to the appropriate level

8. Wait approximately 2-2.5 hours for the air temperature rise to an appropriate level

9. When the gas temperature is approximately 20°C higher than desired fuel cell inlet temperature, start the flow of humidification water into the spray chamber - the flow meter (A-15) should read the lowest possible flow

10. Wait an additional 1-2 hours for the temperature and relative humidity to reach steady state – turn humidification water off (A-13) when RH > 94 percent and turn it on when the RH drops below 90 percent

11. Make any necessary adjustments to the Eurotherm set point or the humidification water flow meter.

Hydrogen

1. Set the hydrogen mass flow to 0 SLPM using the LabVIEW program

2. Plumb air into hydrogen line

3. Turn 3-way valve (H-24) to bypass hydrogen around fuel cell

4. Open exhaust valve (H-31)

5. Change mass flow setting in LabVIEW to desired level

6. Adjust exhaust ball valve to achieve the pre-determined line pressure

7. Adjust globe valve (H-11) on heating-humidifiying module to achieve a differential pressure (H-17) between the line and spray nozzle of approximately 30 psi

8. Change Eurotherm setting to the appropriate level

9. Wait approximately 2-2.5 hours for the air temperature rise to an appropriate level

10. When the gas temperature is approximately 20°C higher than desired fuel cell inlet temperature, start the flow of humidification water into the spray chamber - the flow meter (H-15) should read the lowest possible flow

11. Wait an additional 1-2 hours for the temperature and relative humidity to reach steady state – turn humidification water off (H-13) when RH > 94 percent and turn it on when the RH drops below 90 percent

12. Make any necessary adjustments to the Eurotherm set point or the humidification water flow meter.

Coolant Water

1. Ensure that the coolant water reservoir is filled to the appropriate level

2. Turn on switch at fuse box for 480V power

3. Set the tank temperature to the appropriate level in the LabVIEW program

4. Adjust valves (C- 5 and C-17) to channel water through the coolant system but bypassing the fuel cell

5. Turn on the pump (C-3)

6. Check resistivity of the coolant water

7. Wait 30-60 minutes for the tank to reach the temperature set point

Fuel Cell

1. When the coolant reservoir tank temperature has reached its set point, preheat the stack by turning the 3-way valve (C-17) and opening the ball valve (C-14) to flow water through the stack
2. When the air in the hydrogen line is at the desired conditions, turn off the air flow and set the mass flow to zero
3. Purge system with nitrogen for approximately 25 minutes at a flow rate of 43 SLPM
4. Adjust nitrogen flow to 0.27 SLPM per cell
5. Turn 3-way valve (H-24) to purge the stack with nitrogen for approximately 5 minutes
6. Turn 3-way valve (H-24) back to bypass
7. Stop the flow of nitrogen and plumb hydrogen to the hydrogen line

## Testing

1. Make sure that the hydrogen mass flow is set at zero
2. Open the hydrogen bottle valve and adjust the pressure regulator (H-2) to the desired line pressure
3. Close the hydrogen exhaust valve (H-31)
4. Turn the 3-way valves (H-24, A-24) to direct gas flow into the stack
5. Set the mass flow rates of both gases to the appropriate values
6. Observe the open circuit voltage

7. Set the mass flows to the appropriate levels
8. Set the current in the LabVEIW program to the desired value
9. Burp the system every 30 seconds to 1 minute as needed
10. Wait for the coolant temperature at the fuel cell outlet to reach steady state
11. Adjust the flow rate of city water through the heat exchanger (C-9) if steady coolant temperature is not the desired stack temperature
12. After sufficient data is recorded at current setting, repeat steps 7-10 for the next current level (if the next current setting is less than the present current, reverse steps 7 and 8)

**Shutdown**

1. Slowly ramp the current level to zero
2. Set gas mass flows to zero
3. Close the valve on the hydrogen bottle (H-1)
4. Turn off the air compressor (A-1)
5. Turn off the flow of humidification water for both gases
6. Set Eurotherm controllers to values below room temperature and power off the Eurotherm
7. Turn off the pump (C-3)
8. Close the city water supply ball valve
9. Purge stack with nitrogen at 0.27 SLPM per cell for approximately 10 minutes

10. Turn 3-way valve (C-17) to bypass coolant water around stack

11. When stack voltage is approximately 10 percent of the open circuit voltage, connect a power resistor across the buses to bleed the stack of stored energy

12. Remove the resistor when the stack voltage is less than 0.1 V

13. Turn 3-way valves (H-24, A-24) to bypass gases around stack

14. Close valve on nitrogen bottle

15. Disconnect stack from display board and cap all ports

16. Shut down program

# VITA

The author, Mark Davis, began studies for his bachelor's degree in mechanical engineering at Virginia Tech in 1993. During the 5 years of undergraduate work, he co-oped at the National Institute of Standards and Technology in Gaithersburg, MD for four semesters. After graduating in the spring of 1998, he began work towards his master's degree the following fall. Mr. Davis finished his coursework and research responsibilities for the master's degree in the spring of 2000, and, while making final revisions to this thesis, he moved to Falls Church, VA to start full time employment at NIST.